

001
002
003
004
005
006
007
008
009
010
011
012
013
014
015
016
017
018
019
020
021
022
023
024
025
026
027
028
029
030
031
032
033
034
035
036
037
038
039
040
041
042
043
044
045
046

Microbial symbionts buffer hosts from the demographic costs of environmental stochasticity

Joshua C. Fowler^{1,2*}, Shaun Ziegler³, Kenneth D. Whitney³,
Jennifer A. Rudgers³, Tom E.X. Miller¹

¹*Department of BioSciences, Rice University, Houston, 77005, TX, USA.
²Department of Biology, University of Miami, Miami, 33146, FL, USA.
³Department of Biology, University of New Mexico, Albuquerque, 87131, NM, USA.

*Corresponding author(s). E-mail(s): jcf221@miami.edu;
Contributing authors: shaun.ziegler@gmail.com; whitneyk@unm.edu;
jrudgers@unm.edu; tom.miller@rice.edu;
Phone: 719-359-2960

Author Contributions

J.C.F. contributed to data collection, data analysis, and led manuscript drafting. S.Z. contributed to data collection and manuscript revisions. K.D.W. contributed to research conception, data collection, and manuscript revisions. J.A.R. established transplant plots, contributed to research conception, data collection, and manuscript revisions. T.E.X.M. contributed to research conception, data collection, data analysis, and manuscript revisions.

Data and Code Accessibility

Data will be made accessible as an Environmental Data Initiative package online DOI: [updated here when available](#). Code for all analysis is available through [add github repo](#)

Article Type: Letter

Running Title: Symbiont-mediated demographic buffering

Keywords: stochasticity, demography, symbiosis, mutualism, Epichloë

This file contains: Abstract (XX words), Main Text (XX words), Figures (1-4); Supporting information Methods, Supporting Figures A1-A28, Supplemental Tables S1-S4

047

Abstract

048

Species' persistence in increasingly variable climates will depend on resilience
049 against the fitness costs of environmental stochasticity. Most organisms host
050 microbiota that shield against stressors. Here, we test the hypothesis that, by
051 limiting exposure to environmental extremes, microbial symbionts reduce hosts'
052 demographic variance. We parameterized stochastic models using data from a
053 14-year symbiont-removal experiment including seven grass species that host
054 *Epichloë* fungal endophytes. Endophytes reduced variance in fitness by > 10%, on
055 average. Hosts with "fast" life history traits that lacked longevity as an intrinsic
056 buffer benefited most from symbiont-mediated variance buffering. Under current
057 climate, contributions of variance buffering were modest compared to symbiont
058 benefits to mean fitness. However, simulations of increased stochasticity amplified
059 benefits of variance buffering and made it the more important pathway of
060 host-symbiont mutualism than elevated mean fitness. Microbial-mediated variance
061 buffering is likely an important, yet cryptic, mechanism of resilience in an
062 increasingly variable world.

063

064

065

066

067

068

069

070

071

072

073

074

075

076

077

078

079

080

081

082

083

084

085

086

087

088

089

090

091

092

Introduction	093
	094
	095
	096
	097
	098
	099
	100
	101
	102
	103
	104
	105
	106
	107
	108
	109
	110
	111
	112
	113
	114
	115
	116
	117
	118
	119
	120
	121
	122
	123
	124
	125
	126
	127
	128
	129
	130
	131
	132
	133
	134
	135
	136
	137
	138

139 which symbionts may benefit their hosts instead of or in addition to elevating average
140 fitness, the focus of most previous research.

141 We used a combination of long-term field experiments and stochastic demo-
142 graphic modeling to test the hypothesis that context-dependent benefits of symbiosis
143 buffer hosts from the fitness costs of environmental stochasticity. We used cool-season
144 grasses and *Epichloë* fungal endophytes as a tractable experimental model in which
145 non-symbiotic plants can be derived from naturally symbiotic plants through heat
146 treatment, providing a contrast of symbiont effects that controls for the confounding
147 influence of host genetic background. *Epichloë* endophytes are specialized symbionts
148 growing intercellularly in the aboveground tissue of ~ 30% of *C*₃ grass species [29].
149 These fungi are primarily transmitted vertically from maternal plants through seeds
150 [30]. They produce a variety of alkaloids that can protect host plants from natural
151 enemies [31] and drought stress [32].

152 Over 14 years (2007–2021), we collected longitudinal demographic data on the
153 survival, growth, reproduction, and recruitment of all plants within replicated
154 endophyte-symbiotic and endophyte-free populations at our field site in southern Indiana,
155 USA. Through taxonomic replication (seven host-symbiont species pairs) we
156 aimed to understand whether host life history traits could explain inter-specific vari-
157 ation in the magnitude of demographic buffering through symbiosis. We used this
158 long-term data to parameterize stochastic population projection models in a hierar-
159 chical Bayesian framework. Specifically, we (1) quantified the effect of symbiosis on
160 the mean and variance of host vital rates (survival, growth and reproduction) and fit-
161 ness, (2) evaluated the relationship between host life history traits and the magnitude
162 of symbiont-mediated variance buffering, (3) determined the relative contribution of
163 symbiont-mediated mean and variance effects to host fitness, and (4) projected how
164 increased environmental stochasticity (expected under future climates) changes the
165 importance of variance buffering as a pathway of host-symbiont mutualism.
166

167 Materials and Methods

168 Study site and species

169 This study was conducted at Indiana University's Lilly-Dickey Woods Research and
170 Teaching Preserve (39.238533, -86.218150) in Brown County, Indiana, USA. This site
171 is part of the Eastern broadleaf forests of southern Indiana, where the ranges of many
172 understory cool-season grass species overlap. The experiment focused on seven of these
173 grasses (*Agrostis perennans*, *Elymus villosus*, *Elymus virginicus*, *Festuca subverticil-*
174 *lata*, *Lolium arundinaceum*, *Poa alsodes*, and *Poa sylvestris*), each of which hosts a
175 unique species of *Epichloë* endophyte (Table S1). All are native to eastern North
176 America except the Eurasian species *L. arundinaceum*.
177

178 Endophyte removal, plant propagation, and field set-up

179 Seeds from naturally symbiotic populations of the seven focal host species were col-
180 lected during summer-fall 2006 from Lilly-Dickey Woods and the nearby Bayles Road
181 Teaching and Research Preserve (39.220167, -86.542683). To generate symbiotic (S+)
182

and symbiont-free (S-) plants from the same genetic lineages, seeds from each species
185
were disinfected with a heat treatment described in Table S1 or left untreated. The heat
186
treatment created symbiont-free plants by warming seeds to temperatures at which the
187
fungus becomes inviable but the host seeds can still germinate. Both heat-treated and
188
untreated seeds were surface sterilized with bleach to remove epiphyllous microbes,
189
cold stratified for up to 4 weeks, then germinated in a growth chamber before transfer
190
to the greenhouse at Indiana University where they grew for ~ 8 weeks. We confirmed
191
endophyte status by staining thin sections of inner leaf sheath with aniline blue and
192
examining tissue for fungal hyphae at 200X magnification [33]. We established exper-
193
imental populations with vegetatively propagated clones of similar sizes. By starting
194
the experiment with plants of similar sizes and the same number of unique genotypes,
195
we aimed to limit any potential effects of heat treatments on initial plant growth [34].
196

During the fall of 2007 and spring of 2008, we established 10 3x3 m. plots¹ for *A. perennans*, *E. villosus*, *E. virginicus*, *F. subverticillata*, and *L. arundinaceum* and 18
197
plots for *P. alsodes* and *P. sylvestris*. Half of the plots were randomly assigned to be
198
planted with either symbiotic (S+) or symbiont-free (S-) plants, and initiated with
199
20 evenly spaced individuals labeled with aluminum tags. In spring 2008, we placed
200
plastic deer net fencing around each plot to limit deer herbivory and disturbance;
201
damaged fences were regularly replaced.
202
203
204
205
206
207
208
209
210
211
212
213
214
215
216
217
218
219
220
221
222
223
224
225
226
227
228
229
230

Long-term demographic data collection

Each summer (2008–2021) we censused all individuals in each plot for survival,
206
growth and reproduction, and added new recruits to the census. Plots contained 13.3
207
individuals/m² on average over the course of the experiment. Each census year was a
208
sample of inter-annual climatic variation (n = 14 years, comprising 13 demographic
209
transition years). We censused each species during its peak fruiting stage (May: *Poa*
210
alsodes, *Poa sylvestris*; June: *Festuca subverticillata*; July: *Elymus villosus*, *Elymus vir-*
211
ginicus, *Lolium arundinaceum*; September: *Agrostis perennans*), such that the censuses
212
were pre-breeding and new recruits came from the previous years' seed production.
213
Leaf litter was cleared out of each plot prior to the census, to aid in locating plants.
214
For each plant remaining from the previous year, we determined survival, measured
215
its size as a count of tillers, and collected reproductive data as counts of reproductive
216
tillers and seed-bearing spikelets on all reproductive tillers to a maximum of three.
217
We also tagged all unmarked individuals that were recruits from the previous years'
218
seed production and collected the same demographic data. New recruits typically had
219
one tiller and were non-reproductive. In 2008 and 2009, we took additional counts of
220
seeds per inflorescence for all reproducing individuals in the plots to ground-truth our
221
sub-sample estimates.² For *Agrostis perennans*, we also collected seed counts in 2010.³
222
In 2018, we stopped collecting data for the exotic *L. arundinaceum*, which had very
223
high survival and low recruitment, and consequently very low variation across years.
224
In total across 14 years, the dataset included demographic information for 16,789
225
individual host-plants and 31,216 transition-year observations.
226
227
228
229
230

¹I think they are 3 x 2.5

²I don't know what subsample estimates this sentence is referring to.

³Is this sentence necessary?

231 We expected plots to maintain their endophyte status (symbiotic or symbiont-
232 free) because these fungal symbionts are almost exclusively vertically transmitted, and
233 plots were spaced a minimum of 5 m apart, limiting seed dispersal or horizontal trans-
234 mission of the symbiont between plots. However, we regularly confirmed endophyte
235 treatment throughout the lifetime of the experiment by opportunistically taking sub-
236 sets of seeds from reproductive individuals and scoring them for their endophyte status
237 with microscopy as above. Overall, these scores reflected 98% faithfulness of recruits
238 to their expected endophyte status across species and plots (Fig. S23; Supplement
239 data). Additionally, we have rarely observed fungal stromata, the fruiting bodies by
240 which *Epichloë* are potentially transmitted horizontally, provided the fly vector is also
241 present [35]. For *A. perennans*, *F. subverticillata*, *L. arundinaceum*, and *P. alsodes*, we
242 never observed stromata. We observed stromata only infrequently for *E. villosus*, and
243 even more rarely for *E. virginicus* and *P. sylvestris* (Table S2). For these species, stro-
244 mata have only been observed on 35, 4, and 6 plants respectively, making up < 0.3%
245 of all censused plants (Supplemental data).⁴

246

247 Vital rate modeling

248

249 Equipped with these demographic data, we fit statistical models for survival, growth,
250 flowering (yes or no), fertility of flowering plants (number of flowering tillers), pro-
251 duction of seed-bearing spikelets (number per inflorescence), the average number of
252 seeds per spikelet, and the recruitment of seedlings from the preceding year's seed
253 production (Fig. S1 - S10).⁵ We fit these vital rates as generalized linear mixed mod-
254 els in a hierarchical Bayesian framework using RStan [36] which allowed us to isolate
255 endophyte effects on vital rate means and variances, borrow strength across species
256 for some variance components, and propagate uncertainty from the individual-level
257 vital rates to population projection models [37]. All vital rate models included random
258 plot and year effects, with separate estimates of year-to-year variance for symbiotic
259 and symbiont-free plants, to quantify the effect of endophytes on inter-annual vari-
260 ance (Fig. S11 - S18).⁶ All parameters were given vague priors [38]. We ran each vital
261 rate model for 2500 warm-up and 2500 MCMC sampling iterations with three chains.
262 We assessed model convergence with trace plots of posterior chains and checked for
263 \hat{R} values less than 1.01, indicating low within- and between-chain variation [39, 40].
264 For those models that showed poor convergence, we extended the MCMC sampling
265 to include 5000 warm-up and 5000 sampling iterations, which was only necessary for
266 seedling growth. We graphically checked vital rate model fit with posterior predictive
267 checks comparing simulated and observed data (Fig. S19-S20).

268 *Survival* - We modeled survival as a Bernoulli process, where the survival (S) of
269 an individual i in plot p and census year t was predicted by the plot-level endophyte
270 status (e), host species (h), size in the preceding census, and the plant's origin status
271 (whether it was initially transplanted or naturally recruited into the plot).

272

273 ⁴Check how Ecology Letters wants supplements or appendices referenced.

274 ⁵Not sure why you are referencing Supp figures here, they seem like results not methods.

275 ⁶Same comment

276

	277
	278
$S_{i,p,e,h,t} \sim Bernoulli(\hat{S}_{i,p,e,h,t})$	(2a) 279
$logit(\hat{S}_{i,p,e,h,t}) = \beta_{0_h} + \beta_1 * origin_i$	(2b) 280
$+ \beta_{2_h} * endoe + \beta_{3_h} * size_{i,t-1} + \tau_{e,h,t} + \rho_p$	(2c) 281
$\tau_{e,h,t} \sim Normal(0, \sigma_{\tau_{e,h}}^2)$	(2d) 282
$\rho_p \sim Normal(0, \sigma_\rho^2)$	(2e) 283
	284
	285

Here, \hat{S} is the survival probability, β_{0_h} is an intercept specific to each host species, β_1 is the effect of the plant's recruitment origin, β_{2_h} is the endophyte effect, β_{3_h} is the size effect, $\tau_{e,h,t}$ is a normally distributed year effect for each species and endophyte status with variance $\sigma_{\tau_{e,h}}^2$, and ρ_p is a normally distributed plot effect with variance σ_ρ^2 ($p(e)$ indicates that plot identity is uniquely associated with an endophyte status). We assume that origin effect β_1 and plot-to-plot variance σ_ρ^2 are shared across host species, allowing us to "borrow strength" across the multi-species dataset; other model parameters are unique to host species. We separately modeled the survival of newly recruited seedlings with a similar model but omitting previous size dependence and origin status.

Growth - We modeled plant size in census year t (G) with the same linear predictor for the mean as described for survival. Because we measured size as positive integer-valued counts of tillers, we modeled it with a zero-truncated Poisson-inverse Gaussian distribution. This distribution includes a shape parameter λ_G to account for overdispersion in the data. We additionally modeled the growth of newly recruited seedlings separately with a Poisson-inverse Gaussian model omitting size structure and the plants' origin status as with seedling survival.

Flowering - We modeled whether or not a plant was flowering during the census (P) as a Bernoulli process, with the same linear predictor for the mean as described above for survival except that size dependence for reproductive vital rates was determined by the individual's size during the same census year as opposed to its size during the previous year.

Fertility - For a plant that was flowering during the census, its fertility was the number of reproductive tillers produced (F), which we modeled as a function of size in the same census period with a zero-truncated Poisson-Inverse Gaussian distribution, with the same linear predictor for the mean as described above.

Spikelets per Inflorescence - Spikelet production (K) was recorded as integer counts on up to three inflorescences per reproducing plant. We modeled these data with a negative binomial distribution, with the same linear predictor for the mean as described above.

Seed Production per Spikelet - For individuals with recorded counts of seed production, we calculated the number of seeds per spikelet from our counts of seeds and spikelets per inflorescence, and then modeled seeds per spikelet (D) as means of a Gaussian distribution for each species and endophyte status. Because we had less detailed data across years and plants for seed production than for other reproductive vital rates, we omitted both plot and year random effects.

323 *Seedling Recruitment* - We used a binomial distribution to model the recruitment of
 324 new seedlings (R) into the plots from seeds produced in the preceding year, assuming
 325 no long-lived seed bank. We included an intercept specific to each host and endophyte
 326 status and the same random effects structure as in other models. We estimated the
 327 number of seeds per plot in the preceding year by multiplying the total number of
 328 reproductive tillers per plant by the mean number of spikelets per inflorescence and
 329 mean number of seeds per spikelet (D). For plants with missing fertility or spikelet
 330 data, we used the expected number of reproductive tillers (F) or of spikelets per
 331 inflorescence from (K), drawing from the full posteriors of our models. We rounded
 332 this value to get the estimated seed production for each individual, and finally summed
 333 across all reproductive plants in each year and plot to get the total number of seeds
 334 produced.

335

336 **Stochastic population model**

337

338 Using the fitted vital rate models, we parameterized stochastic matrix projection mod-
 339 els including two state variables: r_t (the number of newly recruited individuals in year
 340 t), and \mathbf{n}_t (a vector including all non-seedling individuals of sizes $x \in \{1, 2, \dots, U\}$, rang-
 341 ing from one to the maximum number of tillers U . We use these two state variables to
 342 avoid having to assume demographic equivalence between seedling and non-seedling
 343 one-tiller plants. We used the same model structure for each species and endophyte
 344 status (not shown in model notation, to make it more readable).

345 The number of recruits in year $t + 1$ is given by:

346

$$347 \quad r_{t+1} = \sum_{x=1}^U P(x; \boldsymbol{\tau}_P) F(x; \boldsymbol{\tau}_F) K(x; \boldsymbol{\tau}_K) D R(\boldsymbol{\tau}_R) n_t^x \quad (3)$$

348

349 The total number of seeds produced by a maternal plant of size x is the product
 350 of the size-specific probability of flowering P , the number of reproductive tillers F ,
 351 the number of spikelets per inflorescence K , and the number of seeds per spikelet D .
 352 Multiplying by the probability of transitioning from seed to seedling R gives a per-
 353 capita rate of seedling production, which is multiplied by the number of plants of size
 354 x (n_t^x , the x^{th} element of \mathbf{n}_t) and summed over all sizes. Each function also depends
 355 on the species- and endophyte-specific year random effects for that vital rate ($\boldsymbol{\tau}$, a
 356 vector of year-specific values derived from the statistical models).

357

358 The number of y -sized plants in year $t + 1$ is given by:

359

$$360 \quad n_{t+1}^y = Z(y; \boldsymbol{\tau}_Z) B(\boldsymbol{\tau}_B) r_t + \sum_{x=1}^U S(x; \boldsymbol{\tau}_S) G(x, y; \boldsymbol{\tau}_G) n_t^x \quad (4)$$

361

362 where n_{t+1}^y is the y^{th} element of vector \mathbf{n}_{t+1} . The first term on the right hand side of
 363 Eqn. 4 represents growth (Z) and survival (B) of seedling recruits. The second term
 364 includes the survival of previously x -sized plants and the growth of survivors from size
 365 x to y , summed over all x . To avoid predictions of unrealistic growth outside of the
 366 observed size distribution, we set a ceiling on the growth function for plants at the
 367 97.5th percentile of observed sizes for each host species [41].

Each of the vital rate functions in Eqns. 3 and 4 have separate intercepts and year random effects for symbiotic and symbiont-free populations, allowing us to calculate the effect of endophyte symbiosis on the mean, variance, and coefficient of variation (CV) of λ , the dominant eigenvalue of the year- and endophyte-specific projection matrix. This model treats climate drivers implicitly through year-specific random effects. We also developed a climate-explicit version with the addition of parameters defining the relationship between either annual or growing season drought index and each vital rate. A full description of climate-explicit methods can be found in the Supporting Information Text.

Life History Analysis

We collected metrics describing each host species' life history to test the relationship between pace of life and variance buffering (Table S1). Using the Rage package [42], we calculated R_0 , longevity, and generation time from our estimated transition matrices using the symbiont-free mean matrix as the reference condition. We recorded seed size as the average lemma length from the Flora of North America [43]. We also calculated the 99th percentile of maximum observed age for each species from their S- populations. Next, we fit Bayesian phylogenetic mixed-effects models using the brms package [44] to test the relationship between each life history trait and the effect of symbiosis on the CV of λ (a measure of variance buffering) while controlling for phylogenetic non-independence between host (Fig. 26) and symbiont (Fig. S27) species. We pruned species-level phylogenies of plants[45] and *Epichloë* fungi [46] to include the focal species. *Agrostis perennans* was not included in the tree, and so we used the congener *A. hyemalis*. We defined separate phylogenetic covariance matrices for each pruned tree. We propagated uncertainty in the estimated variance buffering effect V with a measurement error model:

$$\begin{aligned}
 V_{MEAN,h} &\sim Normal(V_{EST,h}, V_{SD,h}) & (5a) \\
 V_{EST,h} &\sim Normal(\mu_h, \sigma) & (5b) \\
 \mu &= \alpha + \beta * trait + \pi & (5c) \\
 \alpha &\sim Normal(0, .5) & (5d) \\
 \beta &\sim Normal(0, .1) & (5e) \\
 \sigma &\sim Half - Normal(.04, .01) & (5f) \\
 \pi &\sim Normal(0, \sigma_\pi * \mathbf{A}) & (5g) \\
 \sigma_\pi &\sim Half - Normal(0, .1) & (5h)
 \end{aligned}$$

Here, V_{EST} is the variance buffering effect for host species h , estimated from the posterior mean (V_{MEAN}) and standard deviation (V_{SD}), propagating uncertainty associated with the effect of symbiosis. The model includes an intercept (α) and a slope (β) defining the relationship between the variance buffering effect and the life history trait. The residual standard deviation is given by (σ). We used weakly informative

415 priors to aid model convergence. Each prior was centered at zero, except for the residual
416 standard deviation, which we centered at the standard deviation of the estimated
417 variance buffering effect, .04. The phylogenetic random effect (π) has a standard deviation
418 (σ_π) which is structured by the covariance matrix A .⁷ We ran each MCMC
419 sampling chain for 8000 warmup iterations and 2000 sampling iterations. We assessed
420 model convergence as described for the vital rate models.

421

422 Mean-variance decomposition

423 To calculate stochastic population growth rates (λ_s) for each host species and endophyte
424 status we simulated population dynamics for 1000 years by randomly sampling
425 from the 13 annual transition matrices, discarding the first 100 years to minimize
426 the influence of initial conditions. Sampling observed transition matrices produces
427 models that realistically capture inter-annual variation by preserving correlations
428 between vital rates [47]. We tallied the total population size at each time step as
429 $N_t = r_t + \sum_{x=1}^U n_t^x$ and calculated the stochastic growth rate as $\log(\lambda_s) = E[\log(\frac{N_t}{N_{t+1}})]$
430 [48, 49]. We calculated the total effect of endophyte symbiosis as the difference in λ_s
431 between S+ and S- populations. We propagated uncertainty from the vital rate models
432 to the calculation of λ_s using 500 draws from the posterior distribution of model
433 parameters.

434 We decomposed the total endophyte effect on λ_s into contributions from effects
435 on vital rate means, variances, and their interaction. Specifically, we repeated the
436 calculation of λ_s for two additional “treatments”: (1) endophyte effects on mean vital
437 rates only, with inter-annual variances shared between S+ and S- at the S- reference
438 level for all vital rates, and (2) endophyte effects on vital rate variances only, with
439 vital rate means shared between S+ and S- at the S- reference level. The combination
440 of all four λ_s treatments (S+ vital rate means and variances, S- means and variances,
441 S+ means with S- variances, S- means with S+ variances) allowed us to quantify to
442 what extent the overall effect of symbiosis derives from changes in vital rates means,
443 variances, and their interaction. The interaction occurs because the variance penalty
444 to stochastic growth is proportional to the mean value of annual growth rates (see Eq.
445 1) such that variance is more detrimental for populations with lower average growth
446 rates.

447 To create scenarios of increased variance relative to that observed during the study
448 period, we repeated the stochastic growth rate decomposition, but sampling only a
449 subset of the 13 observed annual transition matrices. We created two scenarios of
450 increased environmental variance by sampling the transition matrices associated with
451 the six or two most extreme λ values, representing the six or two best and worst years,
452 using S- populations as the reference condition. By sampling away from an average
453 year in both directions, the six- and two- years scenarios increased the standard deviation
454 of yearly host growth rates by 1.3 and 2.1 times, respectively, without changing
455 mean growth rates (< 2.3% difference in $\bar{\lambda}$ between simulation treatments, Fig. S21).
456 We performed the same mean-variance decomposition for these scenarios as for the
457

458
459 ⁷I don't really know these methods so I trust you have thought through this, but equation 5g is not
460 a coherent statistical statement. You are multiplying a scalar times a matrix, which gives a matrix. Is pi
actually a vector and the distribution should be MVN?

ambient conditions (all 13 years sampled) for all host species described above (Fig. S22).⁸

Results and Discussion

⁹

Symbionts buffer host demographic variance

Across seven host species, eight vital rates, 14 years, and 16,789 individual plants, our analysis provided the first empirical evidence of symbiont-mediated variance buffering. Endophytes reduced inter-annual variance for 66% (37/56) of host species-vital rate combinations (average Cohen's D for effects on vital rate standard deviation: -0.15) (Fig 1A). Endophytes also increased mean vital rates for the majority (36/56) of host species-vital rate combinations (average Cohen's D for effects on vital rate mean: 0.15), and benefits were particularly strong for host survival, plant growth and recruitment (Fig. 1A). The magnitude of mean and variance effects differed among host species and vital rates. For example, endophytes modestly increased mean adult survival (Fig. 1C) and reduced variance in survival (Fig. 1D) for *Festuca subverticillata*, while for *Poa alsodes*, variance buffering was more apparent in seedling growth and inflorescence production (Fig 1E). Interestingly, certain vital rates showed costs of endophyte symbiosis. Symbiotic individuals of *A. perennans* grew larger than those without endophytes (Fig. 1B), yet endophytes also reduced this species' mean recruitment rates (Fig. 1A). In addition, endophyte symbiosis increased variance in seedling growth for *Elymus villosus* and *Festuca subverticillata* (Fig. 1A).

Because not all vital rates contribute equally to fitness, we used stochastic matrix models to integrate the diverse effects on vital rates described above into comprehensive measures for the mean and variance of year-to-year fitness (λ_t) and the long-run stochastic fitness that integrates both mean and variance (λ_S). On average across host species, S+ populations had greater mean fitness (> 92% confidence that endophytes increased $\bar{\lambda}$) and lower inter-annual variability in fitness (> 86% confidence that endophytes decreased the coefficient of variation of λ_t) than S- populations (Fig. 2). For some host species, the CV of λ_t declined by as much as 170% (*P. alsodes*, *F. subverticillata*), while for others, endophyte effects on variance were substantially smaller (6% lower for *E. villosus*, 16% lower for *A. perennans*), or even positive (27% increase for *E. virginicus*). When mean and variance effects of symbionts were considered together, none of the host-symbiont pairings were antagonistic (i.e., with endophytes that both decreased mean fitness and increased variance) (Fig. 2C), suggesting that variation across host species and vital rates in mean and variance effects may reflect alternative strategies that yield similar net benefits of endophyte symbiosis.

Reduced sensitivity to drought, as has been reported for some *Epichloë* symbioses [32], is a candidate mechanism that could generate a signature of variance buffering: drought conditions may have weaker fitness costs for S+ hosts, reducing fluctuations in

⁸This might be a holdover from other formats but again, do not reference results figures when you describe methods.

⁹should results and discussion be separate for EL?

507 fitness through time. Accordingly, analysis of climate-explicit matrix models indicated
508 that, for five of seven taxa, S+ populations were less sensitive to annual or growing
509 season drought (12-month or 3- month drought index; Standardized Precipitation-
510 Evapotranspiration Index [50]) than S- populations (Supporting Information Text;
511 Fig. S24-S25; Table S3). However, we did not find a strong relationship between the
512 magnitude of variance buffering and relative drought sensitivities, suggesting that
513 other climatic factors or other temporally-varying aspects of the environment may
514 elicit benefits of endophyte symbiosis, including documented resistance to herbivory
515 for six of these host taxa [51, 52].

516

517 **Faster life histories predict stronger symbiont-mediated 518 variance buffering**

519

520 Theory predicts that long-lived species, those on the slow end of the slow-fast life
521 history continuum, will be less sensitive to environmental variability than short-lived
522 species [53], a pattern which has empirical support across plants [54] and animals
523 [8, 55]. Therefore, host species with long lifespans that produce few, large offspring
524 should benefit less from symbiont-mediated variance buffering than species with fast
525 life cycles that produce many smaller offspring with low per-capita chance of success
526 [56, 57]. In support of this prediction, hosts with trait values representing faster life
527 history strategies experienced greater variance buffering from endophytes than those
528 with slow life histories (Fig. 3). Bayesian phylogenetic mixed-effects models, controlling
529 for species' relatedness, indicated that variance buffering was stronger for host species
530 with shorter lifespan (Fig. 3A; 75% probability of positive relationship with empirically
531 observed maximum plant age) and smaller seeds (Fig. 3B; 73% probability of positive
532 relationship with seed length). Other life history traits similarly had positive, but
533 weaker, support for the prediction that faster life history traits correlate with stronger
534 variance buffering (Fig. S26-S28). Considering fungal life history traits, the three host
535 species for which the net mutualism benefit was weakest (*Elymus villosus*, *Elymus*
536 *virginicus*, and *Poa sylvestris*) (Fig. 2C) were the only hosts for which we observed
537 fungal stromata, fruiting bodies capable of horizontal (contagious) transmission (Table
538 S2). This result supports the theoretical expectation that strict vertical transmission
539 drives the evolution of strong host-symbiont mutualism [20, 58]. Conclusions about
540 life histories are somewhat constrained by the narrow range of trait values among
541 closely related species in the grass sub-family Pooideae and their co-evolving symbionts.
542 Our understanding of how life history variation modulates the fitness consequences of
543 microbial symbiosis would profit from tests across a wider span of taxonomic groups
544 [59].

545

546 **Contributions from variance buffering are weak relative to 547 mean effects**

548

549 To evaluate the relative importance of mean fitness benefits and variance buffering as
550 alternative pathways of mutualism, we decomposed the overall effect of the symbiosis
551 on the stochastic growth rate λ_S using simulations from the population models in four
552 configurations. These included either the full symbiosis effect (both mean and variance

buffering effects), mean effects alone, variance effects alone, or neither mean nor variance effects. Overall, the full effect of symbiosis on λ_S , averaged across host species, provided strong evidence of grass-endophyte mutualism (99% certainty of a positive total effect on λ_s) (Fig. 4; see Fig. S22 for individual host species). Contributions to this full effect derived from both mean and variance buffering effects, as well as a slightly negative interaction (i.e., the combined influence of mean and variance effects was smaller than the sum of their individual effects). Endophytes' contributions to λ_S from mean effects were four times greater, averaged across species, than contributions from variance buffering (Fig. 4), suggesting that, under the regime of environmental variability represented by our 14-year study, damped fluctuations in fitness via variance buffering was a far less important element of the benefits of symbiosis than increased mean fitness. Results for individual host species were largely consistent with the cross-species trends (Fig S22). The full effect of symbiosis on λ_S was positive for seven out of eight host species, with statistical confidence ranging from 66% to 99% certainty. The one exception was the host species *P. sylvestris*, for which our analysis indicated that fungal endophytes were effectively neutral in their overall fitness effect (45% and 55% posterior probability of positive and negative effects; Fig S22).

Variance buffering strengthens under increased environmental variability

Simulations of increased environmental variability, a key prediction of climate change forecasts [2], indicated that mutualism with microbial symbionts, and their variance buffering effects in particular, will take on increased importance for hosts in a more variable future climate. To simulate increased variability, we repeated the decomposition of λ_S for two alternative forecast scenarios, randomly sampling transition matrices that represented either the six most extreme years experienced by each species or the two most extreme years, subsets of the thirteen transition matrices across the 14-year study period. Increased variability elicited stronger mutualistic benefits of endophyte symbiosis (Fig. 3) than ambient variability (overall effect of the symbiosis increased by > 130%). This increase was driven by increased contributions from the variance buffering mechanism (from a 24% contribution in the ambient scenario to a 66% contribution in the most variable scenario) rather than from greater mean effects. In the most variable scenario, the relative importance of mean and variance effects reversed, with variance buffering contributions that were 1.5 times greater than contributions from mean benefits, averaged across species (Fig. 4). Thus, variance buffering – a cryptic microbial influence that manifests only over long time scales – is poised to become the dominant way in which grasses benefit from symbiosis with fungal endophytes in more variable climates of the future.

Conclusion

Ecologists increasingly recognize the importance of symbiotic microbes for host organisms and the populations, communities, and ecosystems in which their hosts reside [60–63]. Despite awareness of these ubiquitous interactions, long-term studies of microbial symbiosis are very rare. Our analysis of taxonomically-replicated, long-term field

599 experiments that manipulated the presence/absence of fungal symbionts in plants
600 demonstrates for the first time that heritable microbes can commonly benefit hosts
601 not only through improved mean fitness – the focus of most previous research – but
602 also through buffering against environmental variance. Our results provide an impor-
603 tant advance to improve forecasts of the responses of populations (and symbiota)
604 to increasing environmental stochasticity under global change, suggesting that, for
605 some host species, microbial symbiosis may compensate for the lack of intrinsic toler-
606 ance of variability conferred by “slow” life history traits. We found that, relative to
607 mean fitness benefits, symbiont-mediated variance buffering made weak contributions
608 to host-symbiont mutualism under the current regime of environmental variability.
609 However, variance buffering is likely to become the dominant benefit that fungal
610 endophytes confer to grass hosts in more variable future environments. This result
611 emerges from the context-dependent nature of grass-endophyte interactions, combined
612 with the observation that environmental stochasticity generates fluctuation in con-
613 text. These key ingredients, and thus the potential for symbiont-mediated variance
614 buffering, similarly apply to the diverse host-microbe symbioses across the tree of life.

615

616

617

618

619

620

621

622

623

624

625

626

627

628

629

630

631

632

633

634

635

636

637

638

639

640

641

642

643

644

Acknowledgments. We thank Mark Sheehan, Ali Campbell, Kyle Dickens, Blaise Willis, and Sar Lindner for contributions to field data collection. We also thank Volker Rudolf, Daniel Kowal, Lydia Beaudrot and Judie Bronstein for helpful comments on and discussion of this project. This research was supported by the National Science Foundation (grants 1754468 and 2208857).	645 646 647 648 649 650 651 652 653 654 655 656 657 658 659 660 661 662 663 664 665 666 667 668 669 670 671 672 673 674 675 676 677 678 679 680 681 682 683 684 685 686 687 688 689 690
Supplementary information. Supplementary information for this paper includes Supplementary Methods, Figs. A1 to A28, and Tables A1 to A3.	

691 **Supplemental Methods**

692 **Estimating climate drivers of environmental context-dependence**

694 To connect the variance buffering effects of endophytes with inter-annual variability
695 in climate, we built climate-explicit stochastic matrix population models from the
696 vital rate data in addition to the climate-implicit model described in the main text.
697 Identifying the potentially complex relationships between vital rates and environmen-
698 tal drivers remains a key challenge for accurate forecasts of the ecological impacts of
699 environmental stochasticity [64]. We first downloaded temperature and precipitation
700 data from a weather station in Bloomington, IN, approx. 27 km from our study site,
701 using the rnoaa package [65]. Compared to other weather stations in the area, the
702 measurements from Bloomington contain the most complete climate record across the
703 study period and are correlated with more local measurements from Nashville, IN for
704 years in which local data are available (total daily precipitation: $R^2 = .76$; mean daily
705 temperature: $R^2 = .94$). The mean annual temperature across the study period was
706 $11.9 C^\circ$ (SD: $1.05 C^\circ$) and the average annual precipitation was 1237.9 mm/year (SD:
707 204.89 mm/year) (Fig. A24). Given the known role of endophytes in promoting host
708 drought tolerance, we calculated the Standardised Precipitation-Evapotranspiration
709 Index (SPEI) for 3 and 12 months preceding each annual censuses, reflecting drought
710 during the growing season and across the year [50]. To calculate SPEI, we used the
711 Thornthwaite equation to model potential evapotranspiration as implemented in the
712 SPEI R package [66]

713 We repeated the process of fitting statistical models for each vital rate as described
714 in **Materials and Methods** with the inclusion of a parameter describing the influ-
715 ence of SPEI. We fit separate vital rate models incorporating either the growing season
716 or annual drought index for each vital rate, except for the model describing the mean
717 number of seeds per inflorescence. This model was fit without climate effects because
718 the data came from only a few years. Initial analyses indicated similar fits for models
719 including only a linear term and those with both linear and quadratic terms describ-
720 ing the relationship between the climate driver and the vital rate response, and so
721 we proceeded with models including only the linear term. We expected that includ-
722 ing climate predictors into the models would explain some inter-annual variance in
723 vital rates, shrinking the variance associated with the fitted year random effects. We
724 assessed model fit with graphic posterior predictive checks and convergence diagnostics
725 as described for the climate-implicit analysis. Finally, we next built matrix projec-
726 tion models incorporating the climate-dependent vital rate functions to assess the
727 response of symbiotic (S+) vs symbiont-free (S-) populations to drought. The model
728 is as described in **Materials and Methods** with the inclusion of parameters describ-
729 ing the slope of the relationship with SPEI. We compared the sensitivity of λ to either
730 annual or seasonal SPEI of S+ populations ($\frac{\Delta\lambda^+}{\Delta SPEI}$) with those of S- populations
731 ($\frac{\Delta\lambda^-}{\Delta SPEI}$) (Fig. S25; Table S).

732 Most species were slightly more responsive to growing season rather than annual
733 drought conditions, and for most species symbiotic populations were less sensitive to
734 SPEI than symbiont-free populations (Fig. S25; Table S3). However, these drought
735 indices did not explain the full extent of inter-annual variability in demographic
736

vital rates. For example, flowering in *A. perennans* had one of the strongest climate signals (82% probability of a positive relationship with SPEI), yet the estimated inter-annual variance $\sigma_{\tau_P}^2$ for symbiont-free plants shrank from 6.7 to 6.1 after including 3-month SPEI as a covariate, suggesting that other factors contribute to inter-annual variability. 737
738
739
740
741
742
743
744
745
746
747
748
749
750
751
752
753
754
755
756
757
758
759
760
761
762
763
764
765
766
767
768
769
770
771
772
773
774
775
776
777
778
779
780
781
782

783 Supplemental Figures A1-A28

784

785

786

787

788

789

790

791

792

793

794

795

796

797

798

799

800

801

802

803

804

805

806

807

808

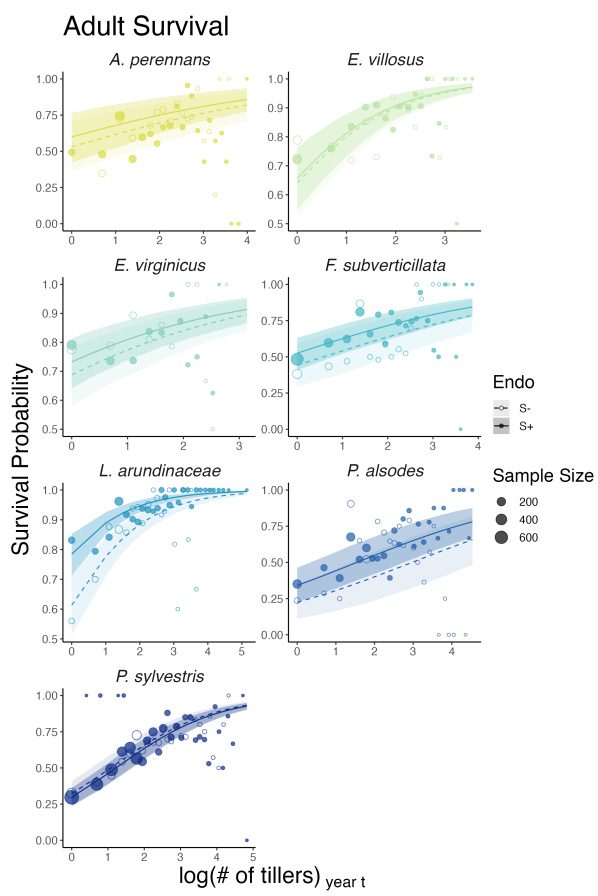
809

810

811

812

813



814 **Fig. 1** Effect of endophyte symbiosis on mean adult survival. Fitted curves represent the size-specific
 815 mean survival probability along with data binned by size shown as open circles with a dashed line
 816 for symbiont-free (S-) plants, while the solid line and filled circles represent symbiotic (S+) plants.
 817 80% credible intervals are shown with dark shading for S+, or light shading for S-.

818

819

820

821

822

823

824

825

826

827

828

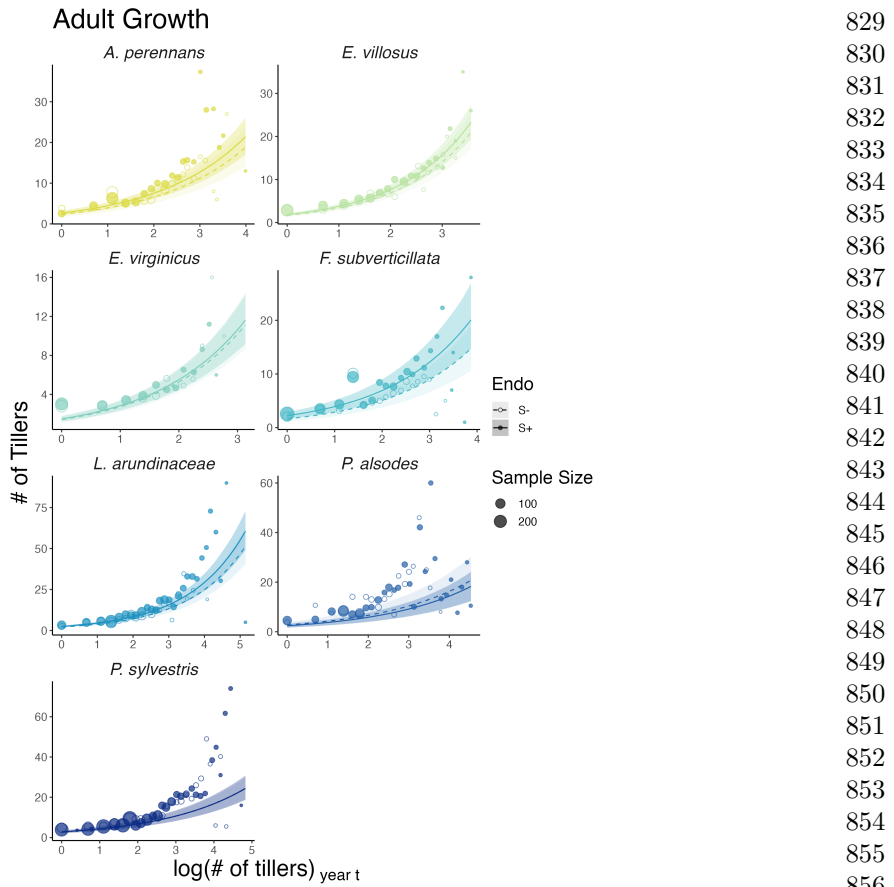
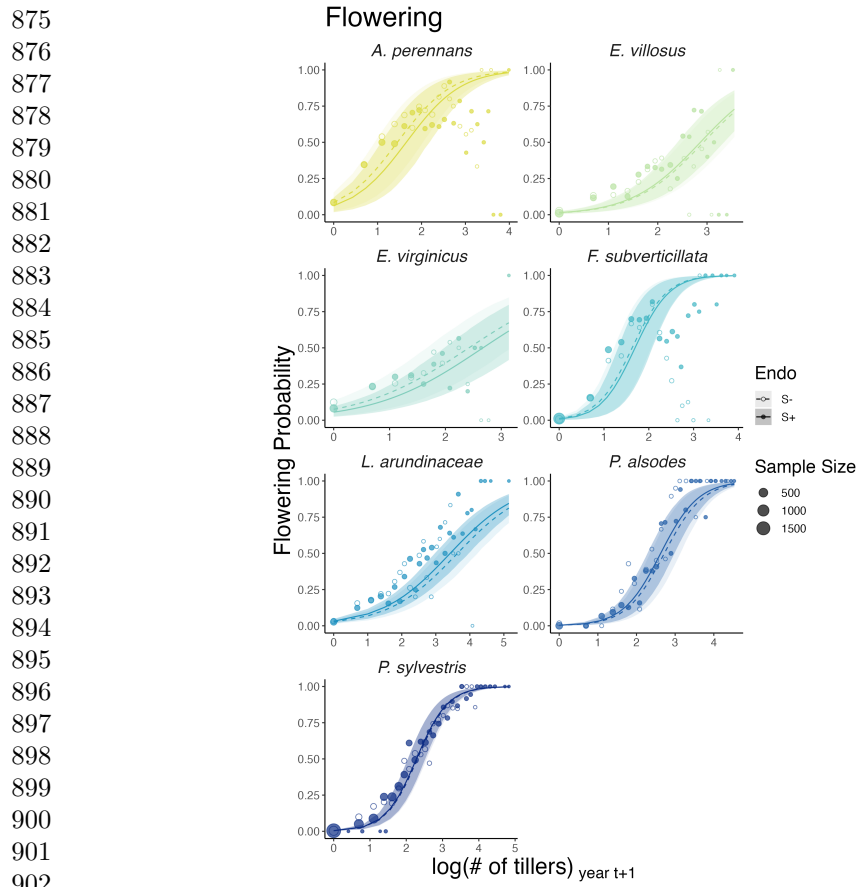


Fig. 2 Effect of endophyte symbiosis on mean adult growth. Fitted curves represent the size-specific mean expected plant size along with data binned by size shown as open circles with a dashed line for symbiont-free (S-) plants, while the solid line and filled circles represent symbiotic (S+) plants. 80% credible intervals are shown with dark shading for S+, or light shading for S-. 829
830
831
832
833
834
835
836
837
838
839
840
841
842
843
844
845
846
847
848
849
850
851
852
853
854
855
856
857
858
859
860
861
862
863
864
865
866
867
868
869
870
871
872
873
874



903 **Fig. 3** Effect of endophyte symbiosis on mean flowering. Fitted curves represent the size-specific
 904 mean flowering probability along with data binned by size shown as open circles with a dashed line
 905 for symbiont-free (S-) plants, while the solid line and filled circles represent symbiotic (S+) plants.
 906 80% credible intervals are shown with dark shading for S+, or light shading for S-.

907
 908
 909
 910
 911
 912
 913
 914
 915
 916
 917
 918
 919
 920

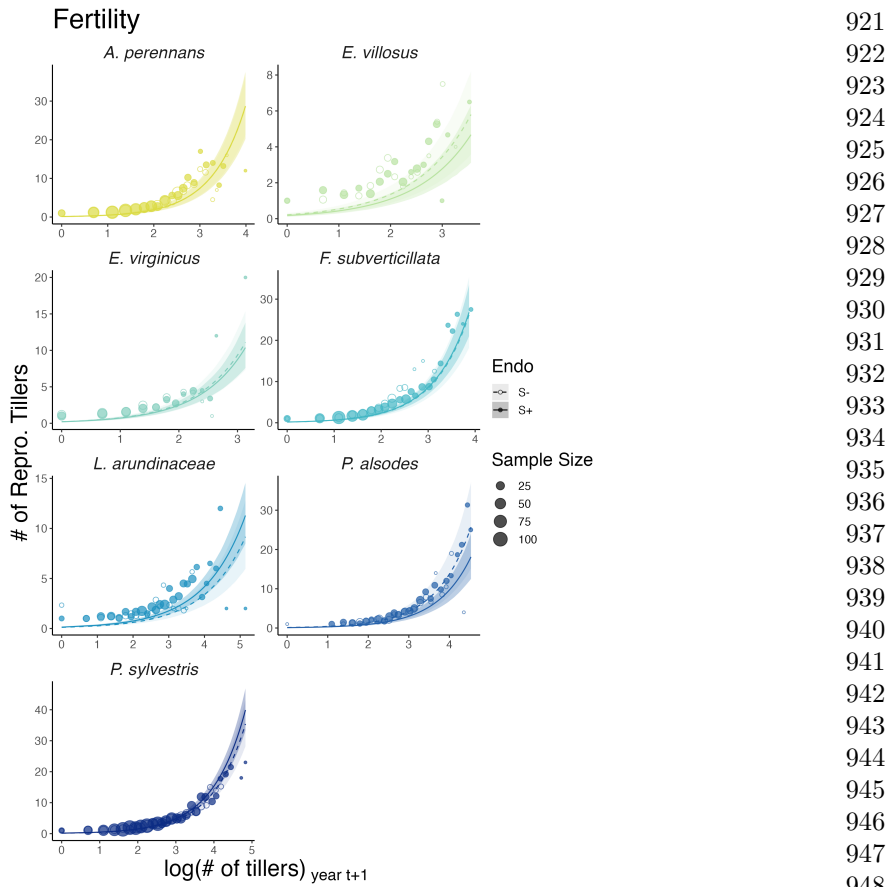
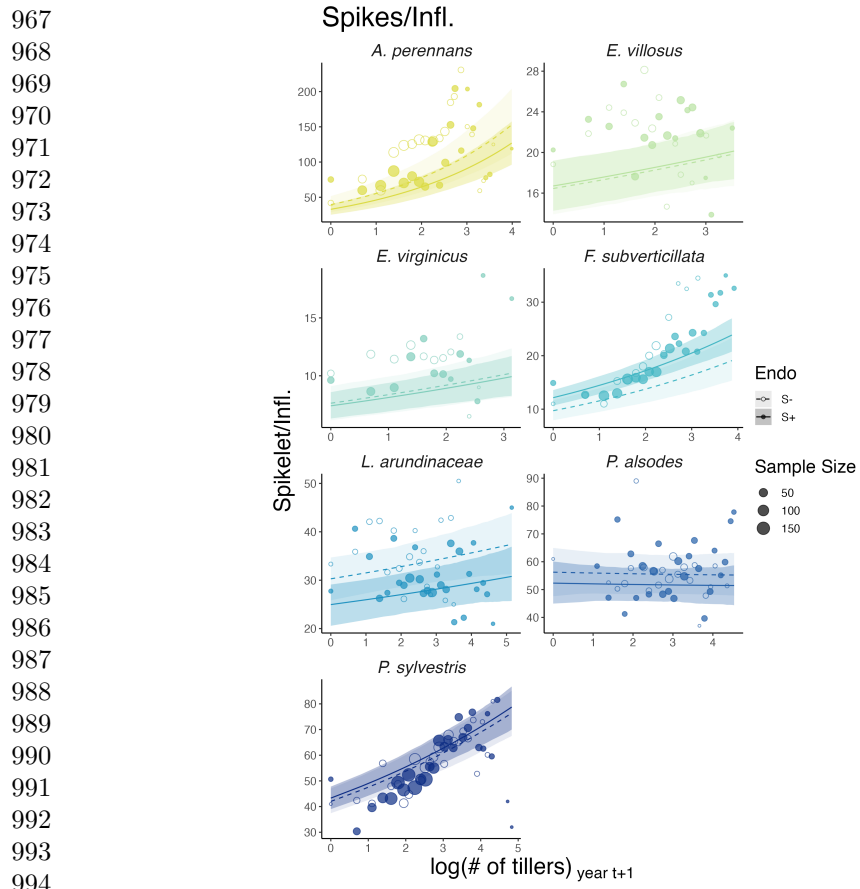


Fig. 4 Effect of endophyte symbiosis on mean fertility. Fitted curves represent the size-specific mean expected number of flowering tillers along with data binned by size shown as open circles with a dashed line for symbiont-free (S-) plants, while the solid line and filled circles represent symbiotic (S+) plants. 80% credible intervals are shown with dark shading for S+, or light shading for S-.



995 **Fig. 5** Effect of endophyte symbiosis on mean spikelet production. Fitted curves represent the size-
 996 specific mean expected number of spikelets per inflorescence along with data binned by size shown
 997 as open circles with a dashed line for symbiont-free (S-) plants, while the solid line and filled circles
 998 represent symbiotic (S+) plants. 80% credible intervals are shown with dark shading for S+, or light
 999 shading for S-.
 1000
 1001
 1002
 1003
 1004
 1005
 1006
 1007
 1008
 1009
 1010
 1011
 1012

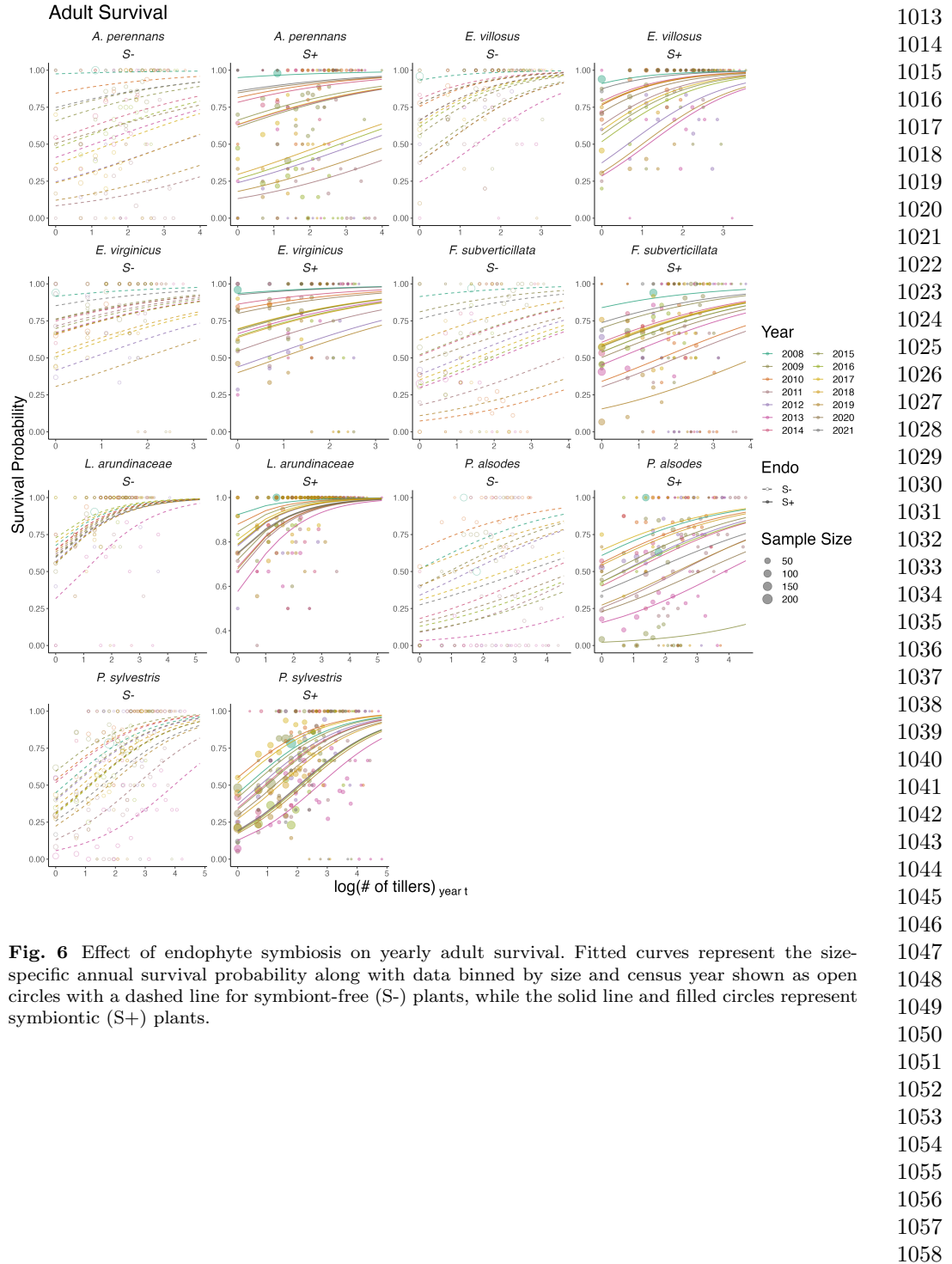
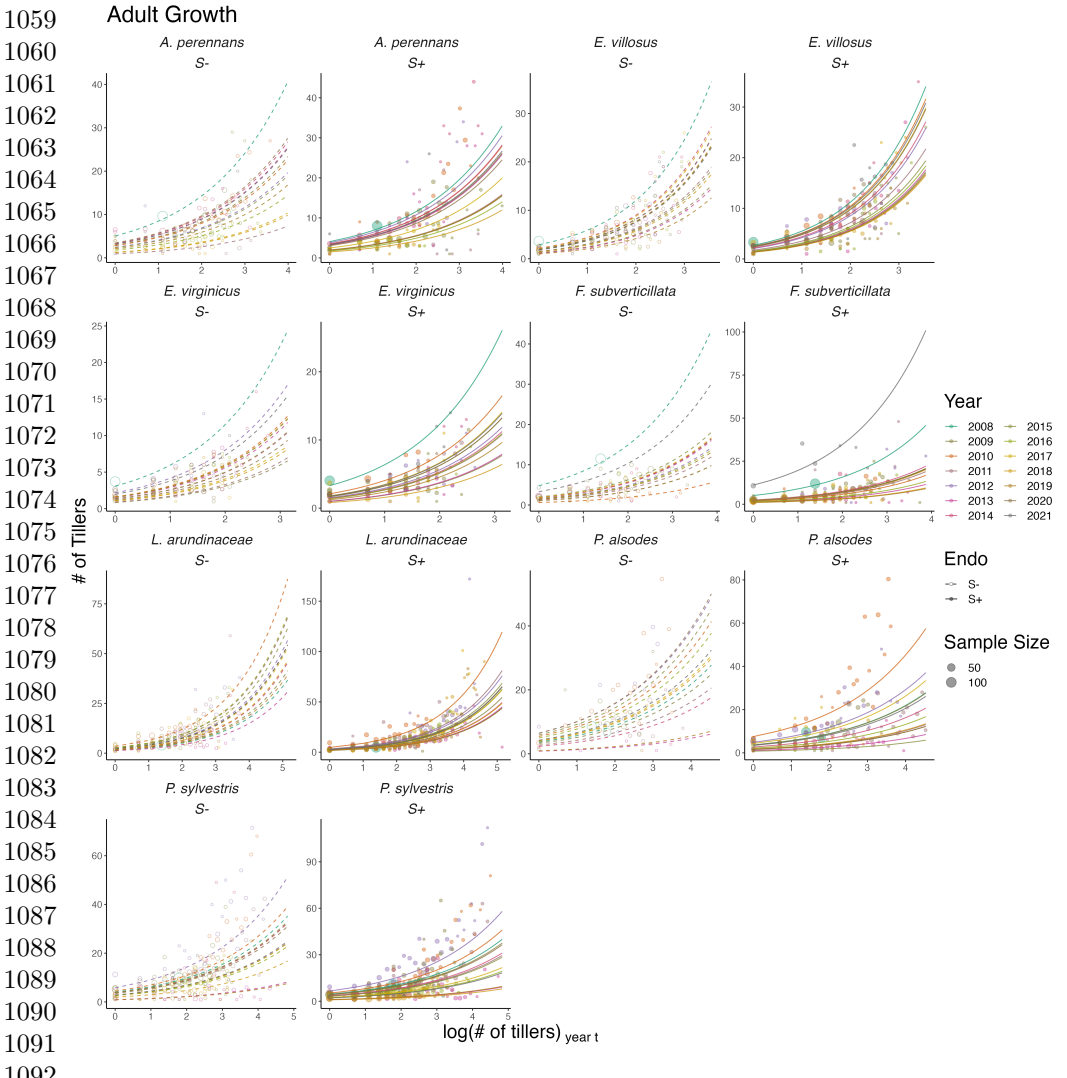


Fig. 6 Effect of endophyte symbiosis on yearly adult survival. Fitted curves represent the size-specific annual survival probability along with data binned by size and census year shown as open circles with a dashed line for symbiont-free (S-) plants, while the solid line and filled circles represent symbiotic (S+) plants.



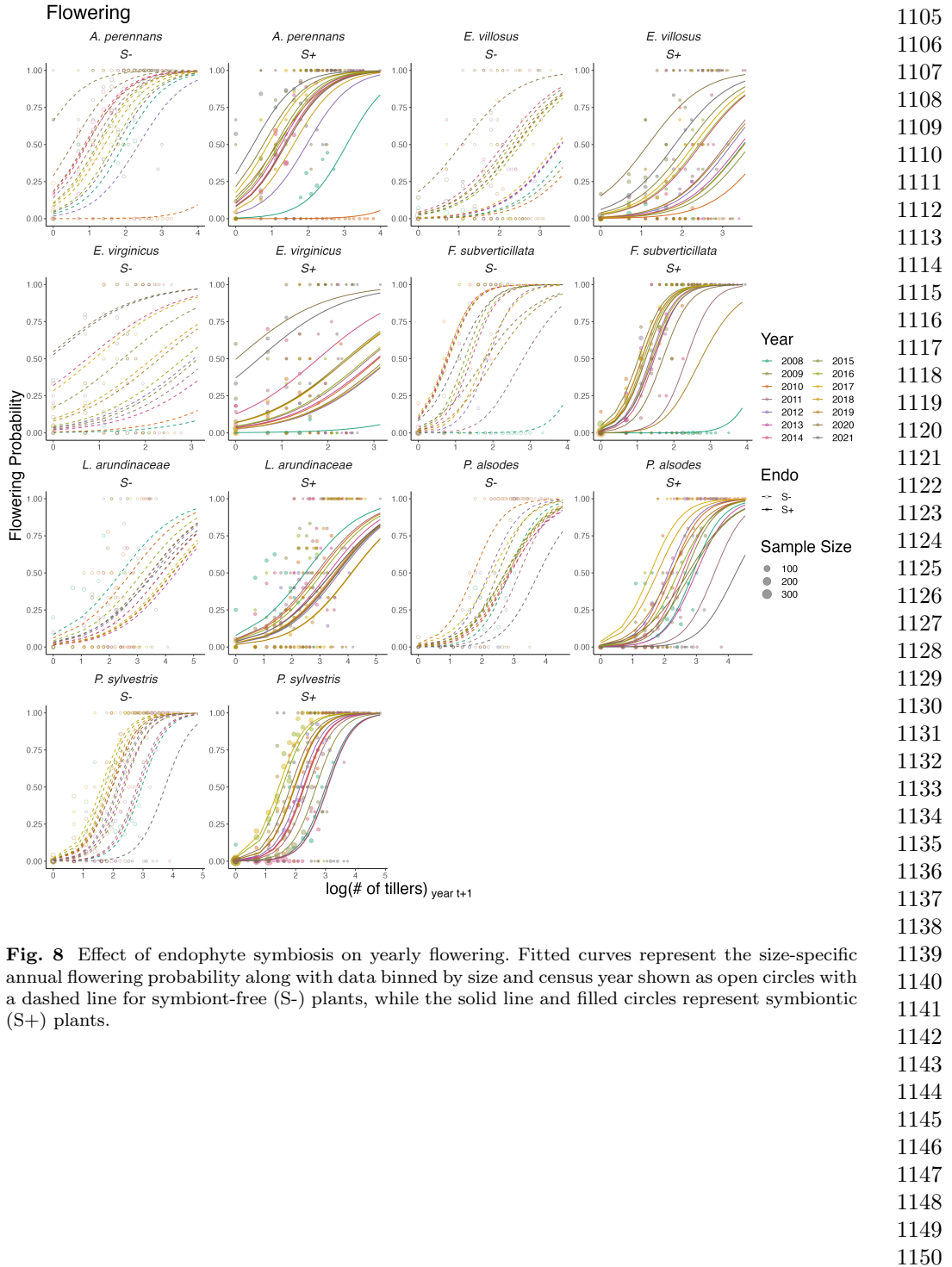
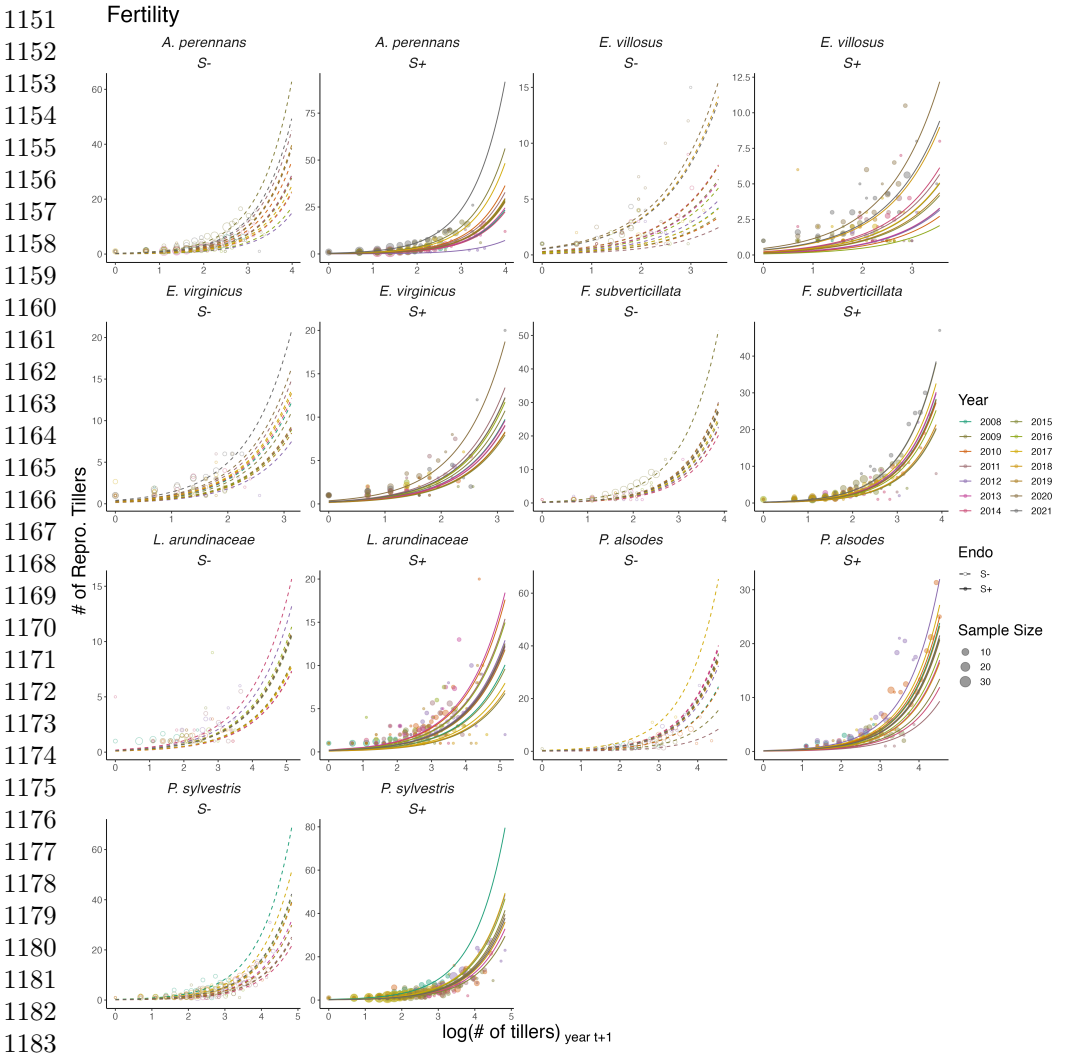


Fig. 8 Effect of endophyte symbiosis on yearly flowering. Fitted curves represent the size-specific annual flowering probability along with data binned by size and census year shown as open circles with a dashed line for symbiont-free (S-) plants, while the solid line and filled circles represent symbiotic (S+) plants.



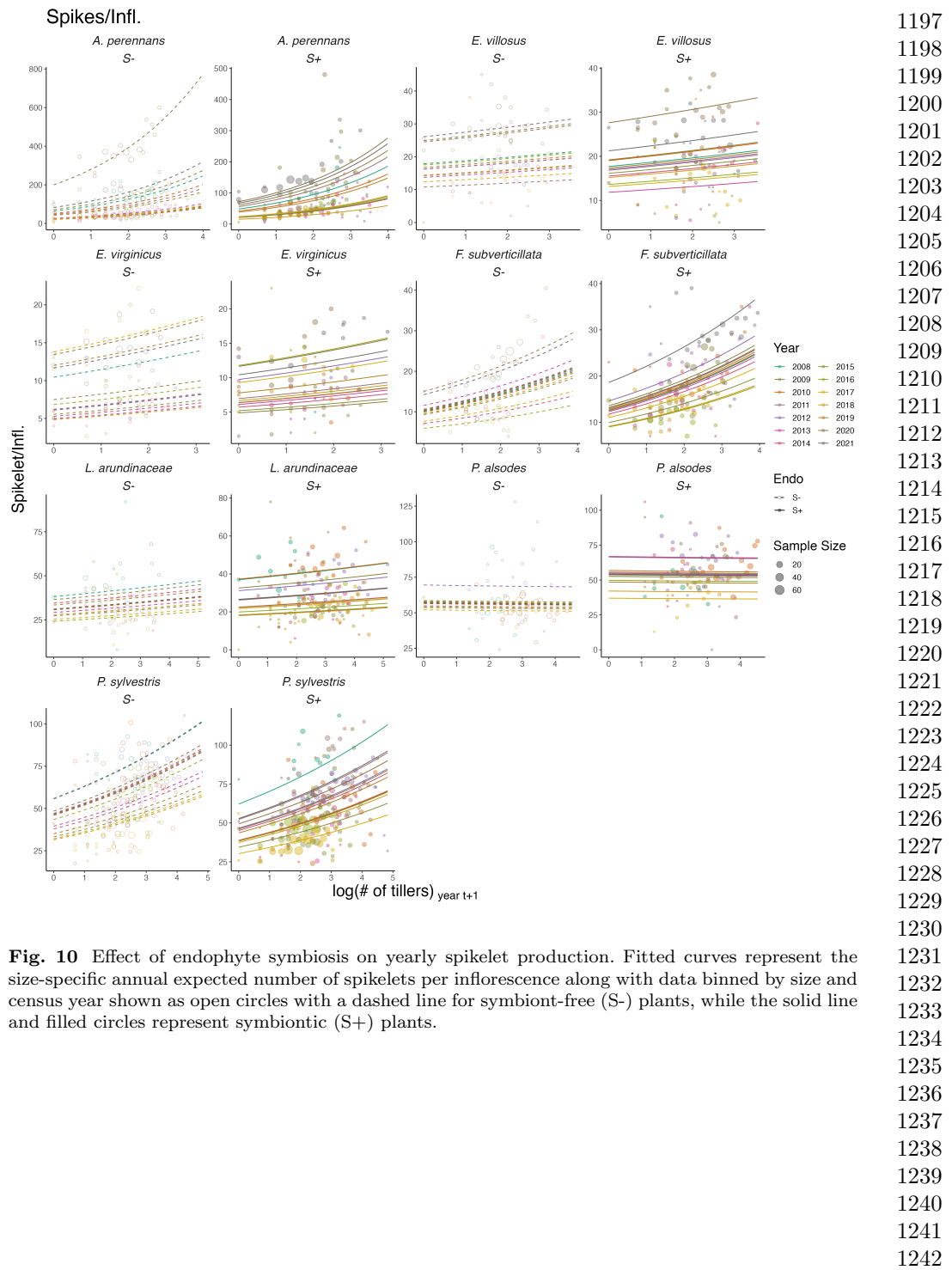
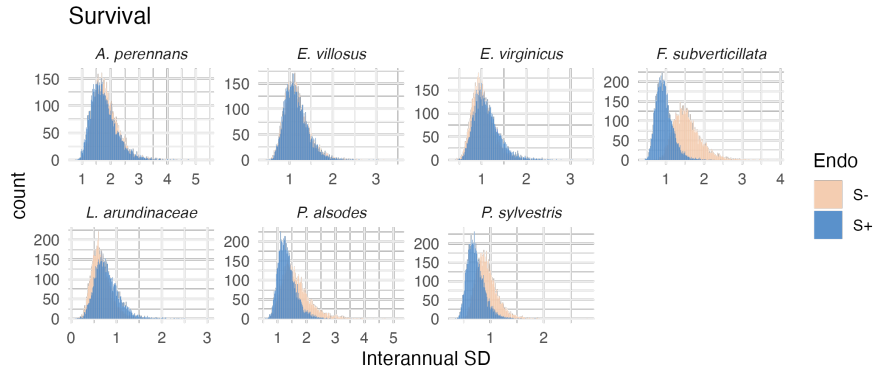


Fig. 10 Effect of endophyte symbiosis on yearly spikelet production. Fitted curves represent the size-specific annual expected number of spikelets per inflorescence along with data binned by size and census year shown as open circles with a dashed line for symbiont-free (S-) plants, while the solid line and filled circles represent symbiotic (S+) plants.



1255 **Fig. 11** Posterior distributions of the standard deviations of inter-annual year effects for survival.
 1256 Histograms include 7500 post-warmup MCMC samples for symbiotic (S+; blue) and symbiont-free
 1257 (S-; tan) plants from fitted vital rate model.

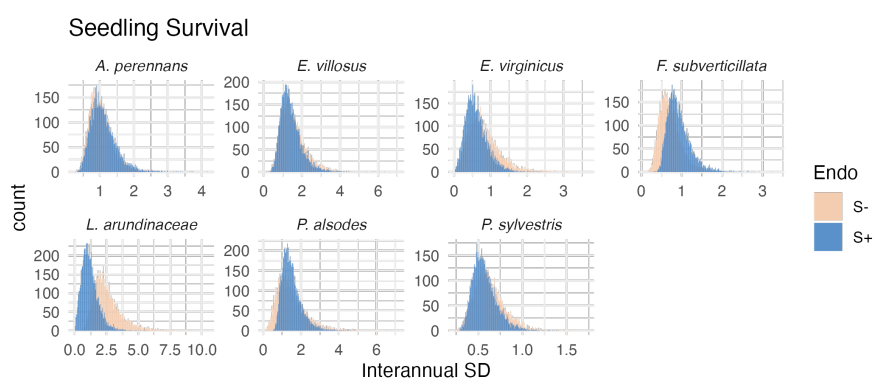


Fig. 12 Posterior distributions of the standard deviations of inter-annual year effects for seedling survival. Histograms include 7500 post-warmup MCMC samples for symbiotic (S+; blue) and symbiont-free (S-; tan) plants from fitted vital rate model.

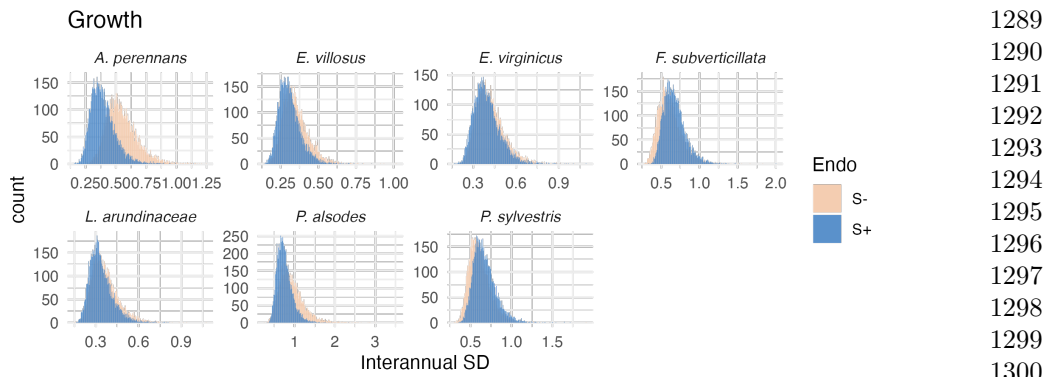


Fig. 13 Posterior distributions of the standard deviations of inter-annual year effects for growth. Histograms include 7500 post-warmup MCMC samples for symbiotic (S+; blue) and symbiont-free (S-; tan) plants from fitted vital rate model.

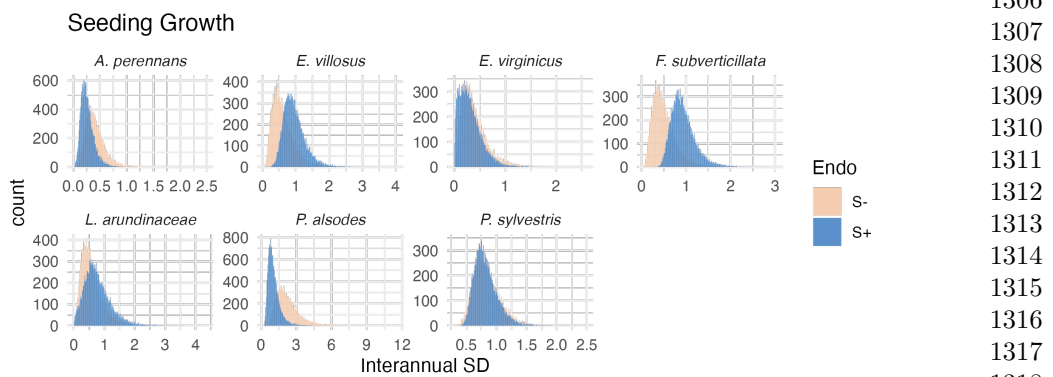


Fig. 14 Posterior distributions of the standard deviations of inter-annual year effects for seedling growth. Histograms include 7500 post-warmup MCMC samples for symbiotic (S+; blue) and symbiont-free (S-; tan) plants from fitted vital rate model.

1308	
1309	
1310	
1311	
1312	
1313	
1314	
1315	
1316	
1317	
1318	
1319	
1320	
1321	
1322	
1323	
1324	
1325	
1326	
1327	
1328	
1329	
1330	
1331	
1332	
1333	
1334	

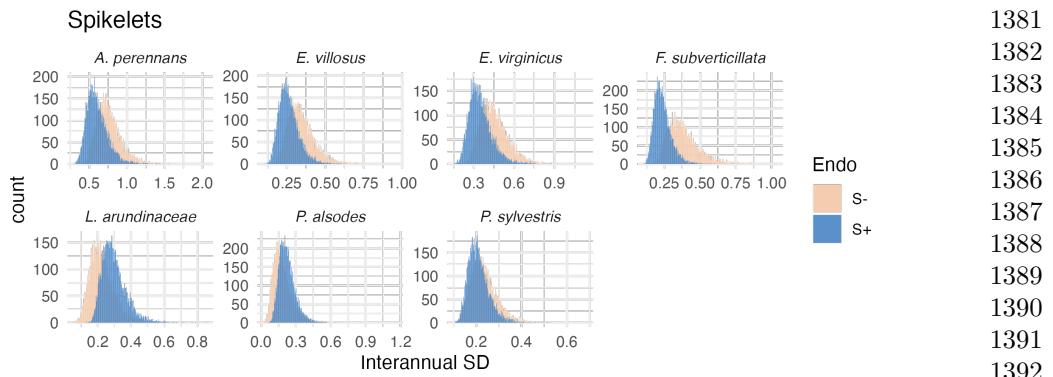


Fig. 17 Posterior distributions of the standard deviations of inter-annual year effects for spikelets per inflorescence. Histograms include 7500 post-warmup MCMC samples for symbiotic (S+; blue) and symbiont-free (S-; tan) plants from fitted vital rate model.

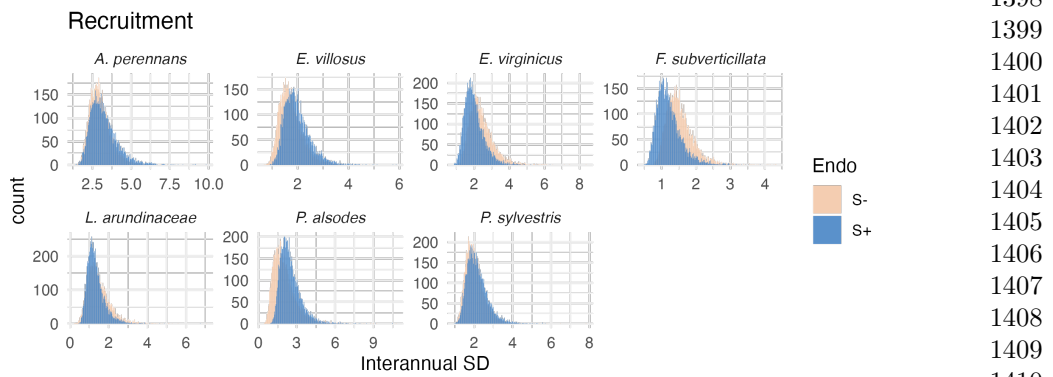
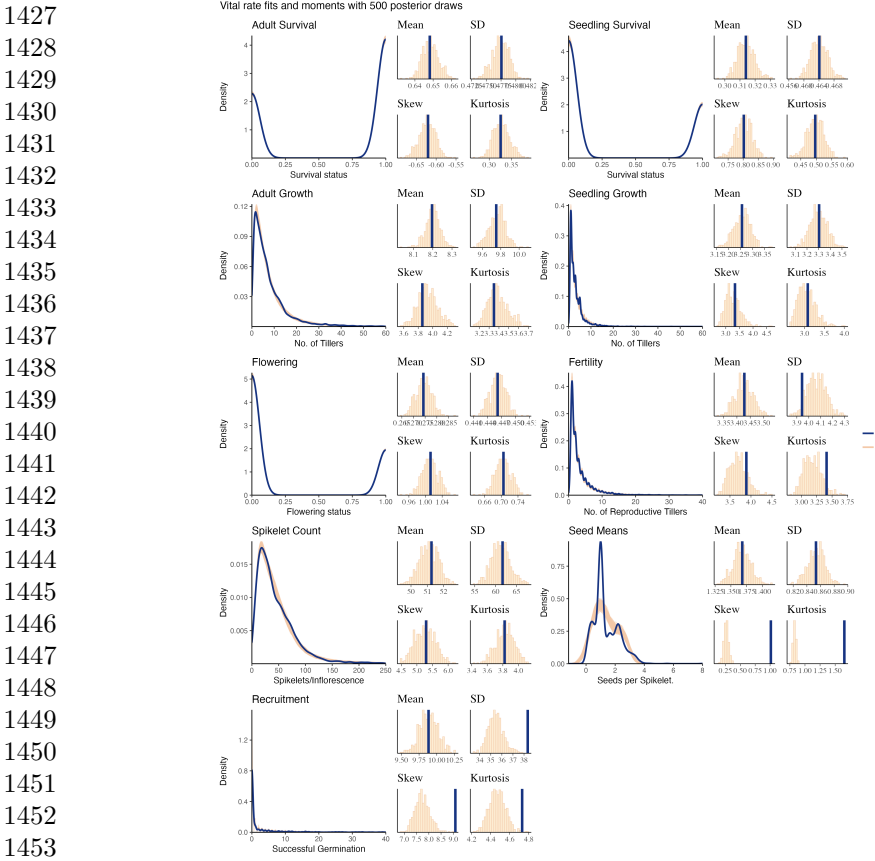


Fig. 18 Posterior distributions of the standard deviations of inter-annual year effects for recruitment. Histograms include 7500 post-warmup MCMC samples for symbiotic (S+; blue) and symbiont-free (S-; tan) plants from fitted vital rate model.

1381
1382
1383
1384
1385
1386
1387
1388
1389
1390
1391
1392
1393
1394
1395
1396
1397
1398
1399
1400
1401
1402
1403
1404
1405
1406
1407
1408
1409
1410
1411
1412
1413
1414
1415
1416
1417
1418
1419
1420
1421
1422
1423
1424
1425
1426



1454 **Fig. 19** Consistency between real data and simulated values indicates that fitted models describe
1455 the data well. Graphs show posterior predictive check for statistical models of demographic vital
1456 rates. Lines show density distributions of observed data (blue line) compared to data simulated from
1457 fitted models (tan lines) generated from 500 draws from posterior distributions of model parameters.

1458
1459
1460
1461
1462
1463
1464
1465
1466
1467
1468
1469
1470
1471
1472

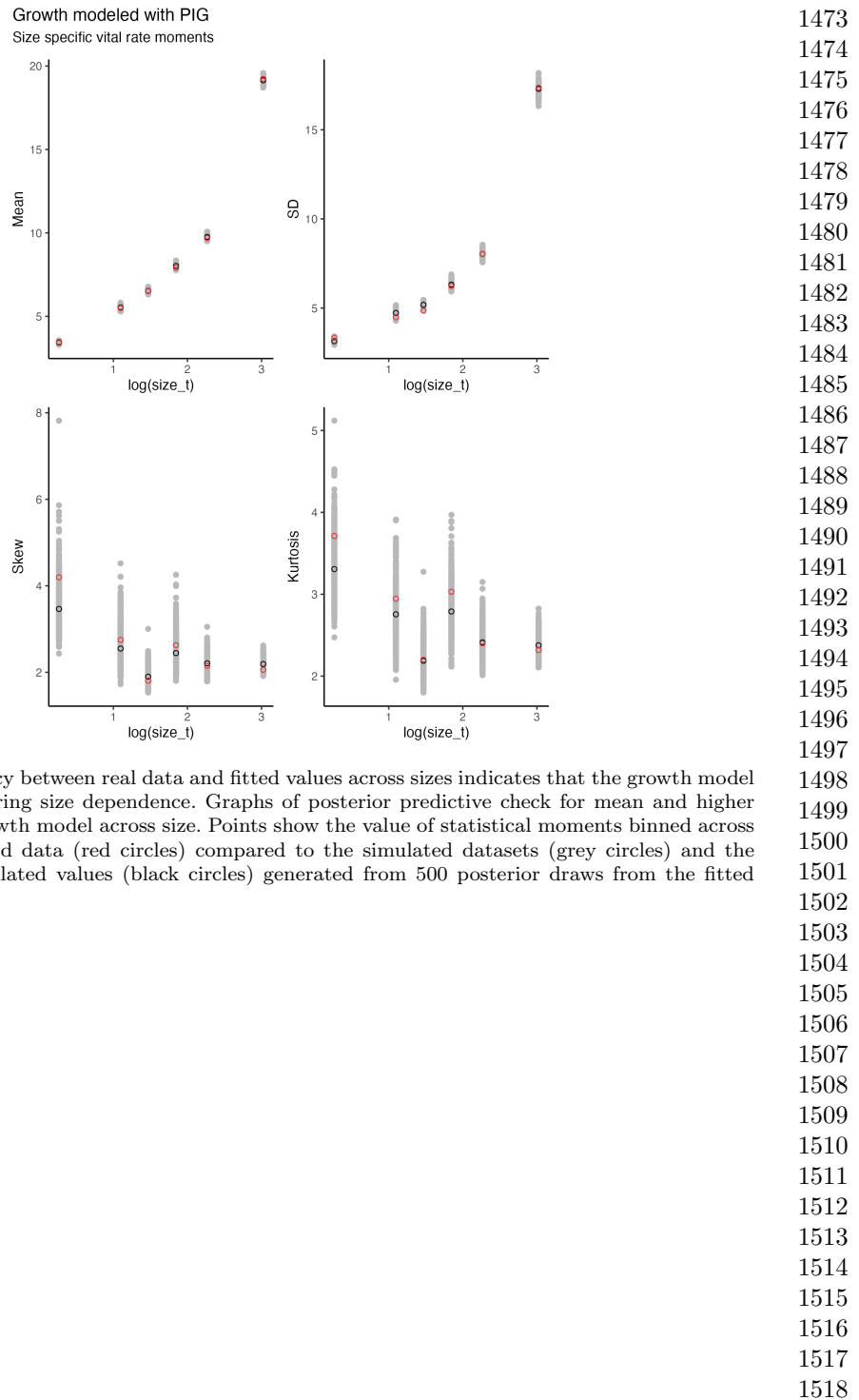
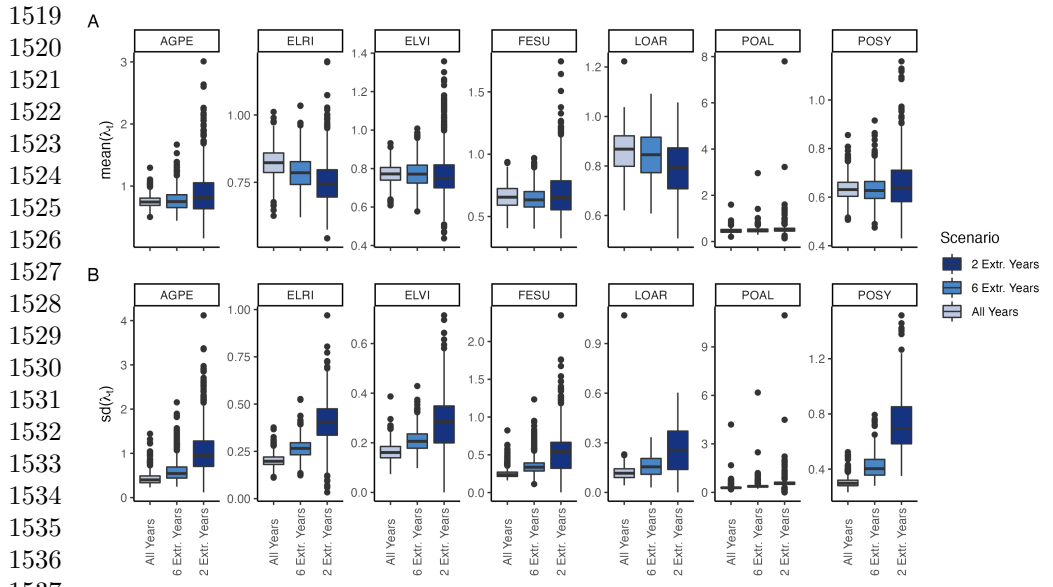
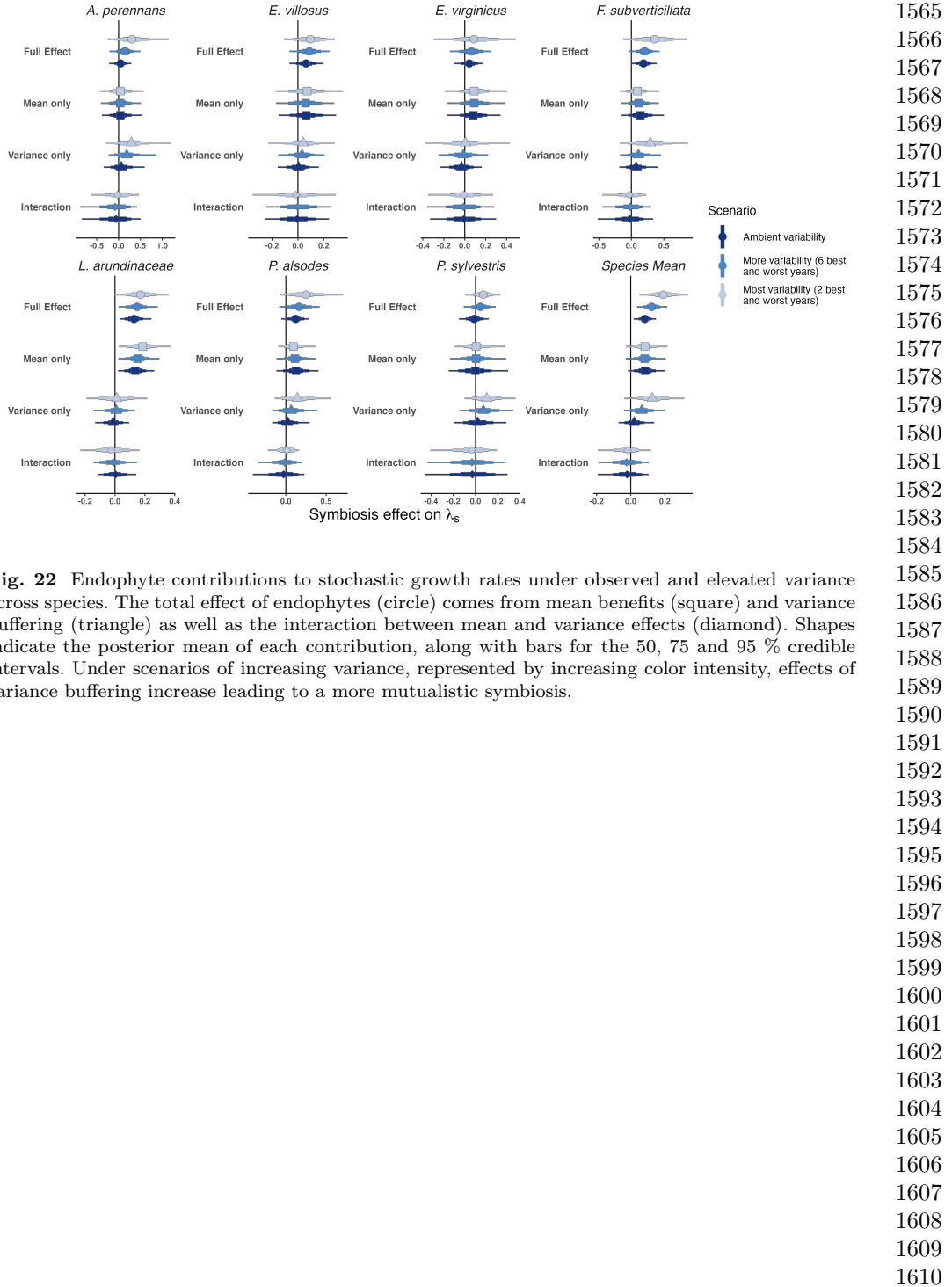
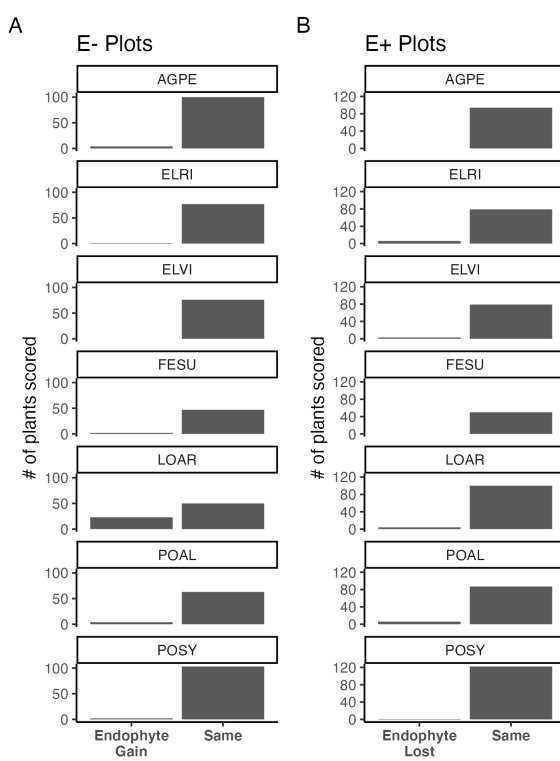


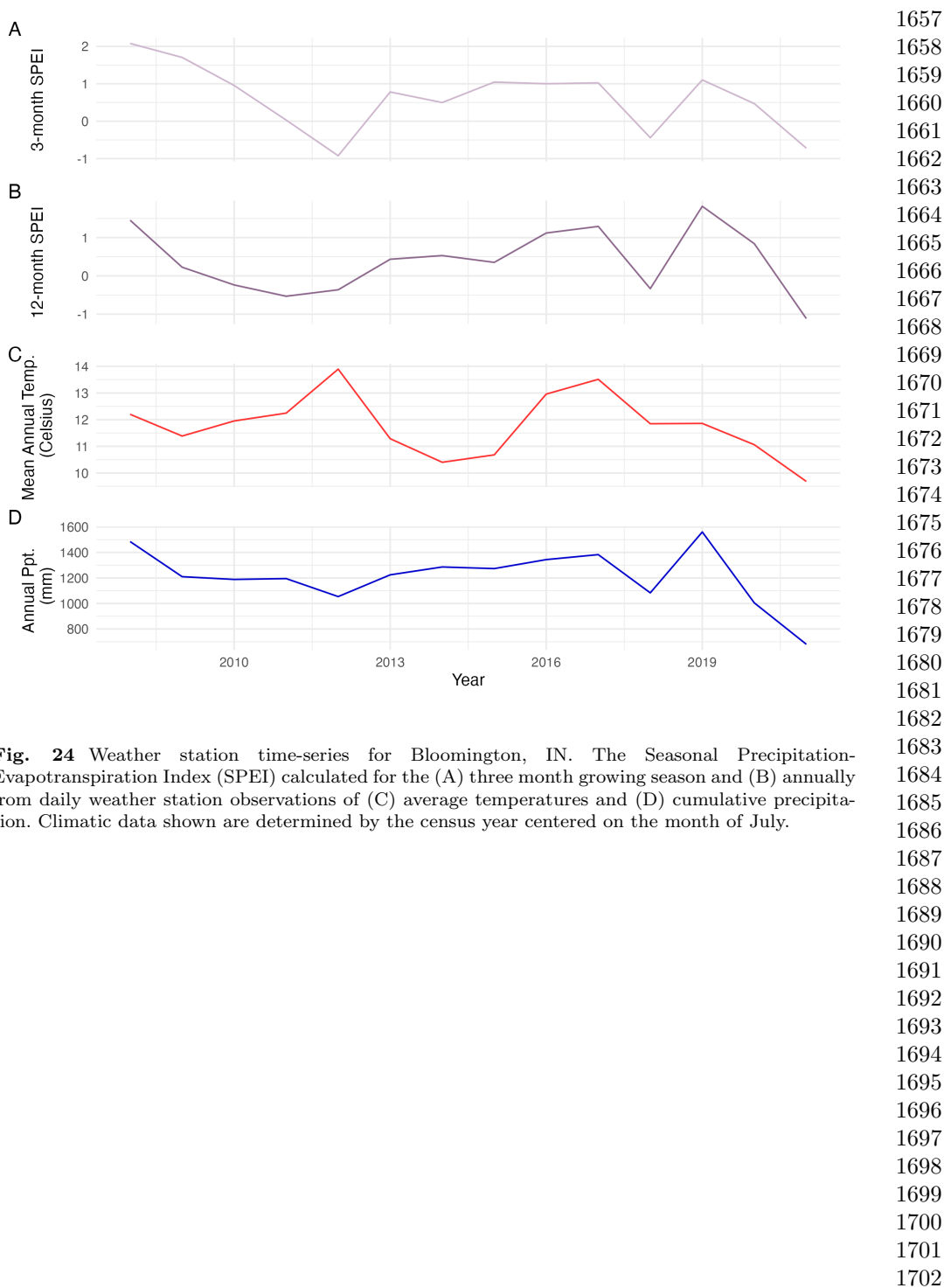
Fig. 20 Consistency between real data and fitted values across sizes indicates that the growth model is accurately capturing size dependence. Graphs of posterior predictive check for mean and higher moments of the growth model across size. Points show the value of statistical moments binned across size for the observed data (red circles) compared to the simulated datasets (grey circles) and the median of the simulated values (black circles) generated from 500 posterior draws from the fitted model.

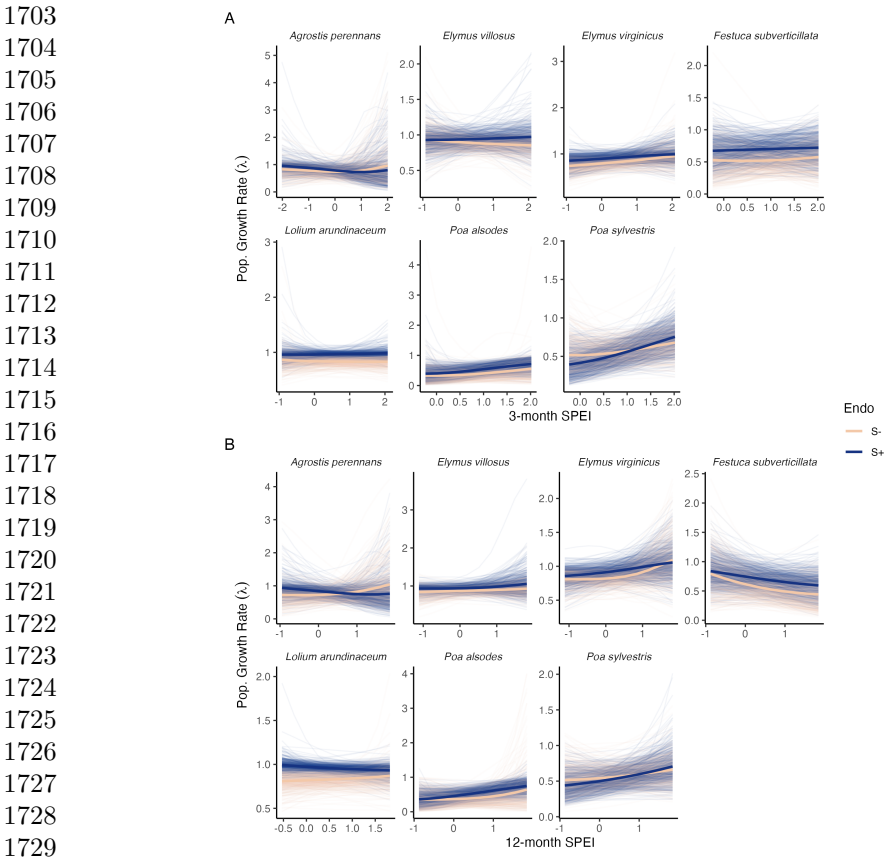




1611
 1612
 1613
 1614
 1615
 1616
 1617
 1618
 1619
 1620
 1621
 1622
 1623
 1624
 1625
 1626
 1627
 1628
 1629
 1630
 1631
 1632
 1633
 1634
 1635
 1636
 1637 **Fig. 23** Endophyte Status Checks
 1638 Counts of plants scored with
 1639 leaf peels or seed squashes to check the faithfulness of recruits to the assigned plot-level endophyte
 1640 status. (A) Endophytic plants may be gained in initially S- plots, or (B) lost in initially S+ plots.
 1641
 1642
 1643
 1644
 1645
 1646
 1647
 1648
 1649
 1650
 1651
 1652
 1653
 1654
 1655
 1656







1730 **Fig. 25** Predicted population growth rates across drought indices. Symbiotic (S+; blue) and
1731 symbiont-free (S-; tan) populations respond differently to climate as measured by the (A) 3-month
1732 SPEI and (B) 12-month SPEI. Thick lines represent the predicted mean growth rate and thin lines
1733 show 500 posterior draws.

1734
1735
1736
1737
1738
1739
1740
1741
1742
1743
1744
1745
1746
1747
1748

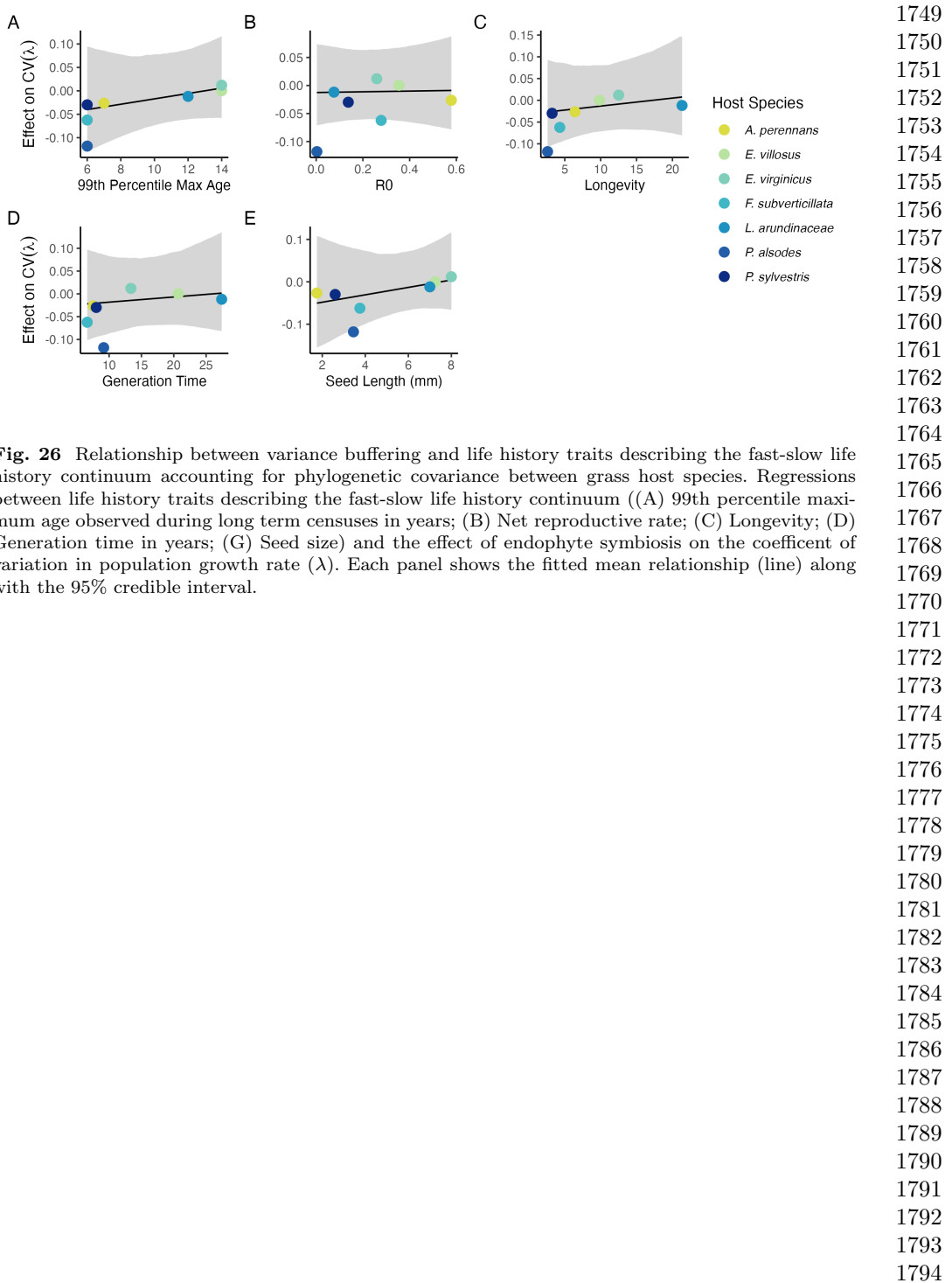


Fig. 26 Relationship between variance buffering and life history traits describing the fast-slow life history continuum accounting for phylogenetic covariance between grass host species. Regressions between life history traits describing the fast-slow life history continuum ((A) 99th percentile maximum age observed during long term censuses in years; (B) Net reproductive rate; (C) Longevity; (D) Generation time in years; (E) Seed size) and the effect of endophyte symbiosis on the coefficient of variation in population growth rate (λ). Each panel shows the fitted mean relationship (line) along with the 95% credible interval.

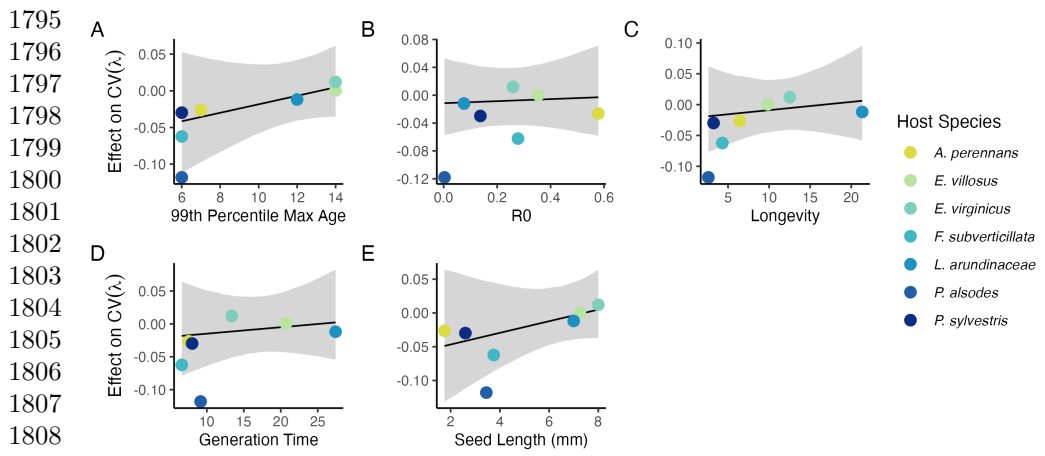


Fig. 27 Relationship between variance buffering and life history traits describing the fast-slow life history continuum accounting for phylogenetic covariance between *Epichloë* symbionts. Regressions between life history traits describing the fast-slow life history continuum ((A) 99th percentile maximum age observed during long term censuses in years; (B) Net reproductive rate; (C) Longevity; (D) Generation time in years; (E) Seed size) and the effect of endophyte symbiosis on the coefficient of variation in population growth rate (λ). Results are similar to regressions accounting for host plant phylogeny (Fig. A25), however symbionts are all within a single genus. Each panel shows the fitted mean relationship (line) along with the 95% credible interval.

1811
 1812
 1813
 1814
 1815
 1816
 1817
 1818
 1819
 1820
 1821
 1822
 1823
 1824
 1825
 1826
 1827
 1828
 1829
 1830
 1831
 1832
 1833
 1834
 1835
 1836
 1837
 1838
 1839
 1840

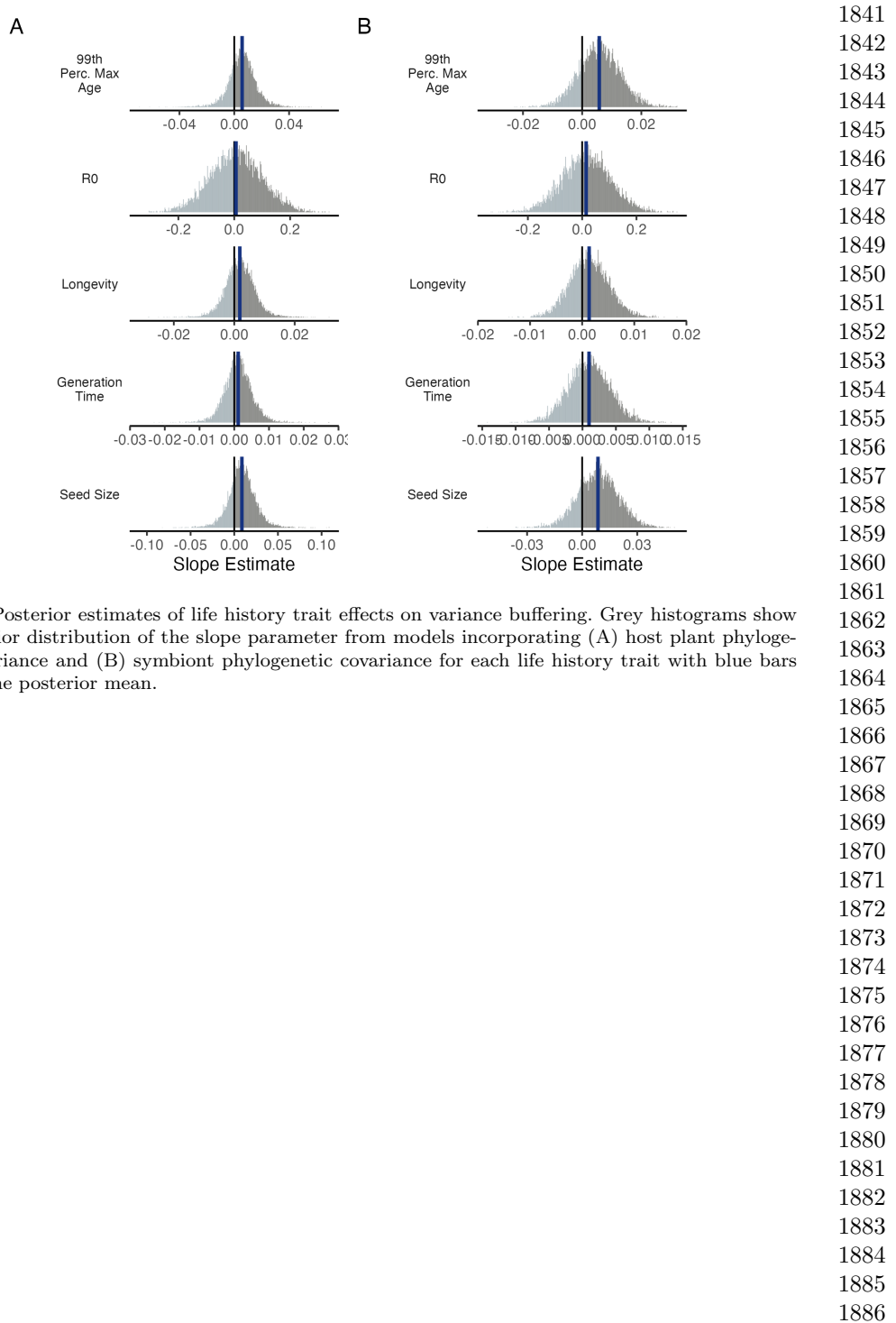


Fig. 28 Posterior estimates of life history trait effects on variance buffering. Grey histograms show the posterior distribution of the slope parameter from models incorporating (A) host plant phylogenetic covariance and (B) symbiont phylogenetic covariance for each life history trait with blue bars showing the posterior mean.

1887 Supplemental Tables A1-A3

1888
1889
1890
1891
1892
1893
1894
1895
1896
1897
1898
1899
1900
1901
1902
1903
1904
1905
1906
1907
1908
1909
1910
1911
1912
1913
1914
1915
1916
1917
1918
1919
1920
1921
1922
1923
1924
1925
1926
1927
1928
1929
1930
1931
1932

1933
1934
1935
1936
1937
1938
1939
1940
1941
1942
1943
1944
1945
1946
1947
1948
1949
1950
1951
1952
1953
1954
1955
1956
1957
1958
1959
1960
1961
1962
1963
1964
1965
1966
1967
1968
1969
1970
1971
1972
1973
1974
1975
1976
1977
1978

Table 1 Summary of host-endophyte propagation and transplant methods

Host Species	Symbiont Species	Heat treatment duration (Temp.)	Transplant date
<i>Agrostis perennans</i>	<i>E. amarillans</i>	12 min. hot water bath (60 °C)	April 2008 (10 plots)
<i>Elymus villosus</i>	<i>E. elymi</i>	6 days drying oven (60 °C)	April 2008 (10 plots)
<i>Elymus virginicus</i>	<i>E. elymi</i> or <i>EviTG-1</i>	6 days drying oven (60 °C)	April 2008 (10 plots)
<i>Festuca subverticillata</i>	<i>E. starrii</i>	6 days drying oven (60 °C)	April 2008 (10 plots)
<i>Lolium arundinaceum</i>	<i>E. coenophiala</i>	6 days drying oven (60 °C)	Sept. 2007 (10 plots)
<i>Poa alsodes</i>	<i>E. alsodes</i>	7 days drying oven (60 °C)	Sept. 2007 (8 plots)/April 2008 (10 plots)
<i>Poa sylvestris</i>	<i>E. PsyTG-1</i>	7 days drying oven (60 °C)	Sept. 2007 (8 plots)/April 2008 (10 plots)

1979
1980
1981
1982
1983
1984
1985
1986
1987
1988
1989
1990
1991
1992
1993
1994
1995
1996
1997
1998
1999
2000
2001
2002
2003
2004
2005
2006
2007
2008
2009
2010
2011
2012
2013
2014
2015
2016
2017
2018
2019
2020
2021
2022
2023
2024

Table 2 Summary of focal life history traits

Host Species	Observed max age (years)	99th percentile max age (years)	Generation time (years)	R ₀	Longevity (years)	Seed length (mm.)	Imperfect transmission rate (%)	Stromata observed of indiv. per species)
<i>Agrostis perennans</i>	11	7	7.6	0.58	6.4	1.75	69.8	0.0
<i>Elymus villosus</i>	14	14	20.7	0.35	9.8	7.25	100	4.6
<i>Elymus virginicus</i>	14	14	13.4	0.25	12.5	8	100	0.6
<i>Festuca subverticillata</i>	9	6	6.6	0.28	4.3	3.75	42.7	0.0
<i>Lolium arundinaceum</i>	12*	12*	27.4	0.08	21.3	7	100	0.0
<i>Poa alsodes</i>	8	6	9.2	0.003	2.6	3.45	99.9	0.0
<i>Poa syvestris</i>	12	6	8.0	0.14	3.2	2.6	16.6	0.1

*Censuses for *L. arundinaceum* plots stopped after year 12 of the experiment.

2025
2026
2027
2028
2029
2030
2031
2032
2033
2034
2035
2036
2037
2038
2039
2040
2041
2042
2043
2044
2045
2046
2047
2048
2049
2050
2051
2052
2053
2054
2055
2056
2057
2058
2059
2060
2061
2062
2063
2064
2065
2066
2067
2068
2069
2070

Table 3 Summary of host-endophyte drought sensitivities

Host Species	Effect on CV(λ)	Effect on Mean(λ)	$\frac{\Delta\lambda^-}{\Delta SPEI_3}$	$\frac{\Delta\lambda^+}{\Delta SPEI_3}$	3 month S- to S+ ratio	$\frac{\Delta\lambda^-}{\Delta SPEI_{12}}$	$\frac{\Delta\lambda^+}{\Delta SPEI_{12}}$	12 month S- to S+ ratio
<i>Agrostis perennans</i>	-0.0264	0.0441	0.03	-0.04	0.85	0.11	-0.06	1.82
<i>Elymus villosus</i>	0.0003	0.0509	-0.03	0.01	1.95	0.03	0.04	0.70
<i>Elymus virginicus</i>	0.0120	0.0578	0.07	0.05	1.50	0.10	0.07	1.42
<i>Festuca subverticillata</i>	-0.0622	0.1639	0.02	0.02	1.01	-0.13	-0.09	1.43
<i>Lolium arundinaceum</i>	-0.0118	0.1022	-0.01	0.01	1.32	0.03	-0.03	1.02
<i>Poa alsodes</i>	-0.1179	0.1282	0.10	0.14	0.71	0.11	0.14	0.73
<i>Poa sylvestris</i>	-0.0298	-0.0085	0.07	0.16	0.44	0.05	0.10	0.55

2071 **References**

- 2072 [1] Seneviratne, S. *et al.* *Changes in climate extremes and their impacts on the*
2073 *natural physical environment* (Cambridge University Press, 2012).
- 2075 [2] IPCC. Climate change 2021: The physical science basis (2021). URL <https://www.ipcc.ch/report/ar6/wg1/>.
- 2076 [3] Lewontin, R. C. & Cohen, D. On Population Growth in a Randomly Varying Envi-
2077 *ronment. Proceedings of the National Academy of Sciences* **62**, 1056–1060 (1969).
2078 URL <https://www.pnas.org/content/62/4/1056>. Publisher: National Academy of
2079 Sciences Section: Biological Sciences: Zoology.
- 2080 [4] Tuljapurkar, S. D. Population dynamics in variable environments. III. Evolution-
2081 *ary dynamics of r-selection. Theoretical Population Biology* **21**, 141–165 (1982).
2082 URL <http://www.sciencedirect.com/science/article/pii/0040580982900107>.
- 2083 [5] Cohen, J. E. Comparative statics and stochastic dynamics of age-structured
2084 populations. *Theoretical population biology* **16**, 159–171 (1979).
- 2085 [6] Tuljapurkar, S. *Population dynamics in variable environments* Vol. 85 (Springer
2086 Science & Business Media, 2013).
- 2087 [7] Pfister, C. A. Patterns of variance in stage-structured populations: evolutionary
2088 predictions and ecological implications. *Proceedings of the National Academy of
2089 Sciences* **95**, 213–218 (1998).
- 2090 [8] Morris, W. F. *et al.* Longevity can buffer plant and animal populations against
2091 changing climatic variability. *Ecology* **89**, 19–25 (2008).
- 2092 [9] Compagnoni, A. *et al.* The effect of demographic correlations on the stochastic
2093 population dynamics of perennial plants. *Ecological Monographs* **86**, 480–494
2094 (2016).
- 2095 [10] Ellis, M. M. & Crone, E. E. The role of transient dynamics in stochastic
2096 population growth for nine perennial plants. *Ecology* **94**, 1681–1686 (2013).
- 2097 [11] Rodríguez-Caro, R. C. *et al.* The limits of demographic buffering in coping with
2098 environmental variation. *Oikos* **130**, 1346–1358 (2021).
- 2099 [12] Tuljapurkar, S. & Orzack, S. H. Population dynamics in variable environments i.
2100 long-run growth rates and extinction. *Theoretical Population Biology* **18**, 314–342
2101 (1980).
- 2102 [13] Fieberg, J. & Ellner, S. P. Stochastic matrix models for conservation and
2103 management: a comparative review of methods. *Ecology letters* **4**, 244–266 (2001).
- 2104
- 2105
- 2106
- 2107
- 2108
- 2109
- 2110
- 2111
- 2112
- 2113
- 2114
- 2115
- 2116

- [14] Menges, E. S. Applications of population viability analyses in plant conservation. *Ecological Bulletins* 73–84 (2000). 2117
2118
2119
- [15] Kuparinen, A., Boit, A., Valdovinos, F. S., Lassaux, H. & Martinez, N. D. Fishing-induced life-history changes degrade and destabilize harvested ecosystems. *Scientific reports* **6**, 22245 (2016). 2120
2121
2122
- [16] Hilde, C. H. *et al.* The Demographic Buffering Hypothesis: Evidence and Challenges. *Trends in Ecology & Evolution* **0** (2020). URL [https://www.cell.com/trends/ecology-evolution/abstract/S0169-5347\(20\)30050-1](https://www.cell.com/trends/ecology-evolution/abstract/S0169-5347(20)30050-1). Publisher: Elsevier. 2123
2124
2125
2126
- [17] Rodriguez, R., White Jr, J., Arnold, A. E. & Redman, a. R. a. Fungal endophytes: diversity and functional roles. *New phytologist* **182**, 314–330 (2009). 2127
2128
2129
- [18] McFall-Ngai, M. *et al.* Animals in a bacterial world, a new imperative for the life sciences. *Proceedings of the National Academy of Sciences* **110**, 3229–3236 (2013). 2130
2131
2132
2133
- [19] Funkhouser, L. J. & Bordenstein, S. R. Mom knows best: the universality of maternal microbial transmission. *PLoS biology* **11**, e1001631 (2013). 2134
2135
2136
- [20] Fine, P. E. Vectors and vertical transmission: an epidemiologic perspective. *Annals of the New York Academy of Sciences* **266**, 173–194 (1975). 2137
2138
2139
- [21] Russell, J. A. & Moran, N. A. Costs and benefits of symbiont infection in aphids: variation among symbionts and across temperatures. *Proceedings of the Royal Society B: Biological Sciences* **273**, 603–610 (2006). 2140
2141
2142
2143
- [22] Kivlin, S. N., Emery, S. M. & Rudgers, J. A. Fungal symbionts alter plant responses to global change. *American Journal of Botany* **100**, 1445–1457 (2013). 2144
2145
- [23] Dunbar, H. E., Wilson, A. C. C., Ferguson, N. R. & Moran, N. A. Aphid thermal tolerance is governed by a point mutation in bacterial symbionts. *PLoS biology* **5**, e96 (2007). 2146
2147
2148
2149
- [24] Reyna, R., Cooke, P., Grum, D., Cook, D. & Creamer, R. Detection and localization of the endophyte undifilum oxytropis in locoweed tissues. *Botany* **90**, 1229–1236 (2012). 2150
2151
2152
2153
- [25] Saikkinen, K., Gundel, P. E. & Helander, M. Chemical ecology mediated by fungal endophytes in grasses. *Journal of chemical ecology* **39**, 962–968 (2013). 2154
2155
2156
- [26] Neyaz, M., Gardner, D. R., Creamer, R. & Cook, D. Localization of the swainsonine-producing chaetothyriales symbiont in the seed and shoot apical meristem in its host ipomoea carnea. *Microorganisms* **10**, 545 (2022). 2157
2158
2159
2160
- [27] Chamberlain, S. A., Bronstein, J. L. & Rudgers, J. A. How context dependent are species interactions? *Ecology letters* **17**, 881–890 (2014). 2161
2162

- 2163 [28] Jordano, P. Spatial and temporal variation in the avian-frugivore assemblage of
2164 prunus mahaleb: patterns and consequences. *Oikos* **479–491** (1994).
- 2165
- 2166 [29] Leuchtmann, A. Systematics, distribution, and host specificity of grass endo-
2167 phytes. *Natural toxins* **1**, 150–162 (1992).
- 2168
- 2169 [30] Cheplick, G. P., Faeth, S. & Faeth, S. H. *Ecology and evolution of the grass-*
2170 *endophyte symbiosis* (OUP USA, 2009).
- 2171
- 2172 [31] Brem, D. & Leuchtmann, A. Epichloë grass endophytes increase herbivore resis-
2173 tance in the woodland grass *brachypodium sylvaticum*. *Oecologia* **126**, 522–530
2174 (2001).
- 2175
- 2176 [32] Decunta, F. A., Pérez, L. I., Malinowski, D. P., Molina-Montenegro, M. A. &
2177 Gundel, P. E. A systematic review on the effects of epichloë fungal endophytes
2178 on drought tolerance in cool-season grasses. *Frontiers in plant science* **12**, 644731
2179 (2021).
- 2180
- 2181 [33] Bacon, C. W. & White, J. F. in *Stains, media, and procedures for analyzing*
2182 *endophytes* 47–56 (CRC Press, 2018).
- 2183
- 2184 [34] Rudgers, J. A. & Swafford, A. L. Benefits of a fungal endophyte in *elymus*
2185 *virginicus* decline under drought stress. *Basic and Applied Ecology* **10**, 43–51
2186 (2009).
- 2187
- 2188 [35] Bultman, T. L., White Jr, J. F., Bowdish, T. I., Welch, A. M. & Johnston, J.
2189 Mutualistic transfer of epichloë spermatia by phorbia flies. *Mycologia* **87**, 182–189
2190 (1995).
- 2191
- 2192 [36] Stan Development Team. RStan: the R interface to Stan (2022). URL <https://mc-stan.org/>. R package version 2.21.7.
- 2193
- 2194 [37] Elderd, B. D. & Miller, T. E. Quantifying demographic uncertainty: Bayesian
2195 methods for integral projection models. *Ecological Monographs* **86**, 125–144
2196 (2016).
- 2197
- 2198 [38] Gabry, J., Simpson, D., Vehtari, A., Betancourt, M. & Gelman, A. Visualization
2199 in bayesian workflow. *Journal of the Royal Statistical Society Series A: Statistics*
2200 in Society **182**, 389–402 (2019).
- 2201
- 2202 [39] Brooks, S. P. & Gelman, A. General methods for monitoring convergence of
2203 iterative simulations. *Journal of computational and graphical statistics* **7**, 434–455
2204 (1998).
- 2205
- 2206 [40] Gelman, A. & Hill, J. *Data analysis using regression and multilevel/hierarchical*
2207 *models* (Cambridge university press, 2006).
- 2208

- [41] Williams, J. L., Miller, T. E. & Ellner, S. P. Avoiding unintentional eviction from integral projection models. *Ecology* **93**, 2008–2014 (2012). 2209
2210
2211
- [42] Jones, O. R. *et al.* Rcompadre and rage—two r packages to facilitate the use of the compadre and comadre databases and calculation of life-history traits from matrix population models. *Methods in Ecology and Evolution* **13**, 770–781 (2022). 2212
2213
2214
2215
2216
2217
2218
2219
- [43]
- [44] Bürkner, P.-C. brms: An R package for Bayesian multilevel models using Stan. *Journal of Statistical Software* **80**, 1–28 (2017). 2220
2221
2222
- [45] Zanne, A. E. *et al.* Three keys to the radiation of angiosperms into freezing environments. *Nature* **506**, 89–92 (2014). 2223
2224
2225
2226
- [46] Leuchtmann, A., Bacon, C. W., Schardl, C. L., White Jr, J. F. & Tadych, M. Nomenclatural realignment of neotyphodium species with genus epichloë. *Mycologia* **106**, 202–215 (2014). 2227
2228
2229
2230
- [47] Metcalf, C. J. E. *et al.* Statistical modelling of annual variation for inference on stochastic population dynamics using integral projection models. *Methods in Ecology and Evolution* **6**, 1007–1017 (2015). 2231
2232
2233
2234
2235
- [48] Caswell, H. Matrix population models: Construction, analysis, and interpretation. 2nd edn sinauer associates. Inc., Sunderland, MA (2001). 2236
2237
2238
2239
- [49] Rees, M. & Ellner, S. P. Integral projection models for populations in temporally varying environments. *Ecological Monographs* **79**, 575–594 (2009). 2240
2241
2242
- [50] Vicente-Serrano, S. M., Beguería, S. & López-Moreno, J. I. A multiscalar drought index sensitive to global warming: the standardized precipitation evapotranspiration index. *Journal of climate* **23**, 1696–1718 (2010). 2243
2244
2245
2246
- [51] Rudgers, J. A. & Clay, K. An invasive plant–fungal mutualism reduces arthropod diversity. *Ecology Letters* **11**, 831–840 (2008). 2247
2248
2249
- [52] Crawford, K. M., Land, J. M. & Rudgers, J. A. Fungal endophytes of native grasses decrease insect herbivore preference and performance. *Oecologia* **164**, 431–444 (2010). 2250
2251
2252
2253
2254
- [53] Murphy, G. I. Pattern in life history and the environment. *The American Naturalist* **102**, 391–403 (1968).
- [54] Compagnoni, A. *et al.* Herbaceous perennial plants with short generation time have stronger responses to climate anomalies than those with longer generation time. *Nature communications* **12**, 1–8 (2021).

- 2255 [55] Le Coeur, C., Yoccoz, N. G., Salguero-Gómez, R. & Vindenes, Y. Life his-
2256 tory adaptations to fluctuating environments: Combined effects of demographic
2257 buffering and lability. *Ecology Letters* **25**, 2107–2119 (2022).
- 2258
- 2259 [56] Rees, M. Evolutionary ecology of seed dormancy and seed size. *Philosophical
2260 Transactions of the Royal Society of London. Series B: Biological Sciences* **351**,
2261 1299–1308 (1996).
- 2262
- 2263 [57] Moles, A. T. & Westoby, M. Seedling survival and seed size: a synthesis of the
2264 literature. *Journal of Ecology* **92**, 372–383 (2004).
- 2265
- 2266 [58] Afkhami, M. E. & Rudgers, J. A. Symbiosis lost: imperfect vertical transmission
2267 of fungal endophytes in grasses. *The American Naturalist* **172**, 405–416 (2008).
- 2268
- 2269 [59] Jeschke, J. M. & Kokko, H. The roles of body size and phylogeny in fast and
2270 slow life histories. *Evolutionary Ecology* **23**, 867–878 (2009).
- 2271
- 2272 [60] Afkhami, M. E. & Strauss, S. Y. Native fungal endophytes suppress an exotic
2273 dominant and increase plant diversity over small and large spatial scales. *Ecology*
2274 **97**, 1159–1169 (2016).
- 2275
- 2276 [61] Smith, E., Vaughan, G., Ketchum, R., McParland, D. & Burt, J. Symbiont
2277 community stability through severe coral bleaching in a thermally extreme lagoon.
2278 *Scientific Reports* **7**, 2428 (2017).
- 2279
- 2280 [62] Dallas, J. W. & Warne, R. W. Captivity and animal microbiomes: potential roles
2281 of microbiota for influencing animal conservation. *Microbial Ecology* 1–19 (2022).
- 2282
- 2283 [63] Wu, L. *et al.* Reduction of microbial diversity in grassland soil is driven by
2284 long-term climate warming. *Nature Microbiology* **7**, 1054–1062 (2022).
- 2285
- 2286 [64] Ehrlén, J. & Morris, W. F. Predicting changes in the distribution and abundance
2287 of species under environmental change. *Ecology letters* **18**, 303–314 (2015).
- 2288
- 2289 [65] Chamberlain, S., Hocking, D. & Anderson, B. Package ‘rnoaa’ (2022).
- 2290
- 2291
- 2292
- 2293
- 2294
- 2295
- 2296
- 2297
- 2298
- 2299
- 2300